Effect of Stiffness and Texturing on *Staphylococcus epidermidis* Adhesion to Surfaces

15 May 2020

Mary Cromwick WPI '20

Helena Petroff WPI '22

Contents

Table of Figures

Table of Tables

Acknowledgements

Abstract

The goal of this project was to develop a surface that can resist bacteria biofilm growth using only the physical properties of the surface. Previous research has shown that *Staphylococcus aureus* adhesion decreases as the stiffness of hydrophobic surfaces increases. Other research regarding surface texture showed that micropillars of approximately the same size as *Staphylococcus epidermidis* reduced bacterial adhesion. The team hypothesizes that by combining material properties of high stiffness and surface texture similar to the size of *S. epidermidis*, the surface will reduce bacterial adhesion better than either property by itself.

The team reports preliminary data characterizing the antimicrobial and stiffness properties of surfaces. Additionally, the team describes the experiments planned for D term 2020 and the anticipated results. The research conducted provides information on how stiffness can affect bacterial adhesion. Ultimately this could aid scientists and engineers in the future as they work towards developing anti-fouling surfaces.

1.0 Introduction

1.1 Motivation

1.1.1 Biofilm Complications

Many bacteria are able to form biofilms, which are clusters of cells that stick together, forming an encasing extracellular matrix structure on a surface. After initial adhesion to the surface, the bacteria slowly grow and propagate over time across that surface. Particularly in a nutrient-rich environment, such as the human body, the bacteria can rapidly reproduce. Doing so, the bacteria often harden to the surface, as they irreversibly attach and secrete proteins, minerals, and waste. These biofilms are often formed on any surface that bacteria can easily attach to, particularly medical implants and biomedical devices [1,2].

Bacterial attachment to biomedical devices that are within the body or on surfaces that are in contact with the body, such as surfaces in medical facilities, creates an environment that easily causes clinical infections. Millions of Americans have *in vivo* devices for a multitude of medical diagnoses. Studies have shown that bacterial biofouling results in infections caused by biofilms usually show recurring symptoms, until the surface that the biofilm has grown on is completely removed from the body [2,3]. From microscopic eye surgery to major joint replacements, these devices provide opportunities for bacteria to infiltrate the human body and cause complications [4,5].

Biofilms can cause severe illness after surgery, if the instrumentation or testing devices were contaminated, due to bacterial infection and interference with proper operation of equipment [6]. Bacterial fouling that occurs on *in vivo* implants may cause more harm to the body than if the implant was not in place. The instrumentation has a shorter lifespan and does not interface properly with its environment due to the bacteria buildup on its surface [1,7]. For example, patients that require a folate catheter, which is very common in most in-patient hospitals, must take extra precautions to prevent bacteria from spreading to the area around the catheter. Research has shown that biofilms result in material and structural barriers against physical and mechanical stimuli, allowing bacteria to withstand normally harsh environments and partially resulting in drug resistant bacteria [1,2].

1.1.2 Need for Easily Manufactured Anti-fouling Surfaces

Biofilm formation is affected by the physical, chemical, and structural properties of the surface that the bacteria is interacting with. Previous research reveals that properties such as surface topography, stiffness, and surface functionalization can decrease bacterial cell adhesion by preventing protein absorption and even killing the bacteria [1]. These surfaces, however, are often difficult to manufacture or not feasible for *in vivo* devices for a variety of reasons, including large size or safety. Overall, modification of individual material properties has proven to be the most effective means of limiting bacterial attachment. These include topography, elasticity, hydrophobicity, and stiffness. For example, *S. epidermidis* adhesion is correlated with substrate stiffness. Different strains of bacteria are impacted by surface properties in different ways. [2,8].

The widespread negative effects of bacteria biofilms on substrates involved in patient treatment, including persistent infection and medical device interference, create the need for easily manufacturable surfaces that are anti-fouling. Ready access to vital biomedical implants and sanitary hospital surfaces is necessary

to prevent complications following medical procedures, such as increased risk of further illness. A modified surface that is anti-fouling must be able to be efficiently manufactured and thus readily available to be used with devices that interact with the human body, so that healthcare providers can provide reliable care to those in need [9-11].

1.2 Background

1.2.1 Significance and Clinical Relevance of *S. epidermidis*

Staphylococcus epidermidis is one of the leading causes of healthcare infections, primarily from medical implants [12]. It is commonly found in medical facilities and is endemic to the microbiome of human and animal skin and body tissues [13]. *S. epidermidis* is the primary pathogen in catheter-related bloodstream infections, prosthetic joint complications, and prosthetic valve endocarditis [14]. *S. epidermidis* can be multidrug-resistant and consequently impedes antimicrobial therapy, especially for at-risk individuals, such as those in intensive care units [15]. The infections it causes are chronic due to the persistent biofilms that the bacteria forms on *in vivo* medical devices.

S. epidermidis has several characteristics that make a correct microbial diagnosis and delineation between contamination, colonization, and true infection difficult. For instance, the bacteria is often involved in polymicrobial infections and thus different samplings reveal that a variety of antibiotics for therapy would be beneficial. In addition, the epidemiology and transmission of *S. epidermidis* is little known though it has been recognized as a significant pathogen for over 30 years [16]. There has not been adequate species identification of *S. epidermidis* in a clinical setting, as well as ignorance of the true extent of the bacteria in infections. These issues are primarily due to the fact that the bacteria grows slower than other common species, and so researchers do not always wait to diagnose it in acute infections [17]. The biodiversity and identification issues surrounding infections that involve *S. epidermidis* primarily occur in situations where biofilms are present [12].

Anti-adhesive coatings made from a variety of polymers have been utilized in a clinical setting to prevent *S. epidermidis* adhesion. These nontoxic materials are primarily used to resist protein absorption, and they are also used in combination with antibacterial agents. To prevent colonization, bactericidal substances, including peptides and phosphonium salts are commonly added to the anti-adhesive coating. This dual coating has effective antifouling properties, particularly soon after initial bacterial adhesion [1].

1.2.2 Surface Topography

Bacteria interacts with the substrate it attaches to in a way that is determined by the physical specification of the bacterial species and substrate characteristics. Surface roughness on the nano- and microscales may promote initial bacterial adhesion by providing more surface area for cells to attach to, if the size of the surface features are slightly smaller than the size of the bacteria. Furthermore, other bacteria features such as flagella, may cause the bacteria to better adhere to a rough surface. Consequently, the bacteria shape, as well as length and width, must be taken into consideration when developing substrates that prevent bacterial adhesion [2].

There have been two main approaches to preventing bacterial adhesion of *S. epidermidis* by modification of topography. The first is surface modifications on the nanoscale level. These include pillars with heights below 200 nm, which is significantly less than the size of the bacteria, which has a diameter of approximately 500 – 700 nm [18,19]. This type of surface is often known as a bactericidal surface, as the nanoscale features have been shown to damage the cell wall and kill the bacteria that come into contact with it [19]. It has been speculated that these surfaces reduce adhesion due to their effect on the physicochemical forces (surface free energy), cell membrane deformation, and chemical gradient at the solid–liquid interface [19].

The second approach utilizes micro-features that are roughly the same size as the bacteria. These surfaces are believed to reduce bacterial adhesion by affecting surface hydrodynamics, surface air entrapment, bacteria ordering and segregation on surfaces, and surface conditioning [19]. Due to variability of bacteria shapes and sizes, the optimal size features and spacings may vary considerably between bacteria strains. For example, some studies have shown that a surface topography of hexagons with a unit size of 5 µm and 10 µm tall pillars are ideal for preventing adhesion of *E. coli* [20]. However, studies have shown that *S. epidermidis* adhesion decreases with pillars 0.5 µm to 1 µm in diameter, with spacings approaching the size of the bacteria [21-24].

The shape of the pillar also plays a role in the reduction of bacterial adhesion. Most studies that looked at the adhesion of *S. epidermidis* or *S. aureus* used topographies with circular pillars, however one study found that square pillars were more effective [22]. It is important to note, however, that this study looked at pillars with nanoscale heights as opposed to the micron heights our group would be testing. Our group is therefore looking to test whether this finding holds true for pillars on a micron scale.

1.2.3 Stiffness

Stiffness (or more correctly, elastic modulus) of the surface has also been shown to increase or decrease bacterial adhesion. The correlation depends on whether the material in which stiffness is varied is hydrophobic or hydrophilic. Most studies have demonstrated that bacterial adhesion decreases with decreasing stiffness when the material used is hydrophilic. For example, when the elastic modulus of poly(acrylic acid) (PAA) was varied at values of 1, 20, 40, and 100 MPa, the adhesion of *Escherichia coli* and *S. epidermidis* decreased as the stiffness of PAA decreased [5,33].

The most commonly-used hydrophobic material to test the effects of stiffness on bacterial adhesion is poly(dimethylsiloxane) (PDMS). Its elastic modulus can easily be varied by adjusting the ratio of the base to curing agent, which affects the degree of cross-linking within the material. Previous testing with *S. epidermidis* have commonly used three different ratios of PDMS. Ratios of 5:1, 10:1, 20:1, and 40:1 result in elastic moduli between 0.1 and 2.6 MPa. This range of stiffnesses is similar to those found in biomaterials used for medical applications, such as contact lenses [32].

Research done with hydrophobic materials has shown that bacterial adhesion decreases with increasing stiffness (opposite to the trend on hydrophilic surfaces) [5,32]. The testing that has been done with PDMS and *S. epidermidis* has proven this correlation [34]. Furthermore, the size of attached cells was smaller and the bacteria were less vulnerable to antibiotics including ofloxacin, ampicillin, and tobramycin on the lower stiffnesses of PDMS. Finally, when *Lactococcus lactis* and *E. coli* were grown on poly(l-lysine) (PLL), a hydrophobic material, they grew slower as the stiffness of the substrate increased [33].

The trend is not true in all cases, due to variations in testing procedure and bacteria type. Research showed that as the stiffness of poly(allylamine) hydrochloride (PAH), a hydrophobic surface, decreased, the bacterial attachment of *E. coli* also decreased. It grew about 30 times faster on the substrate that had an elastic modulus of 30 kPa than on the substrate that had an elastic modulus of 150 kPa [5].

The more the stiffness is varied, the more the characteristics of the cells vary from their natural state [34]. Some properties include cell size and susceptibility to antibiotics [35]. Over the course of the research that studies the correlation between substrate stiffness and bacterial adhesion, numerous surface characteristics from varying conditions may cause the overall results to not be consistent [36]. Nevertheless, surface stiffness is a critical material property that influences the response, stress tolerance, and growth of bacteria cells.

1.2.4 Surface Material

Polymers are often used as antibacterial surfaces, either as a coating to prevent bacterial adhesion or a surface that can be easily sterilized. They are primarily used for long-term *in vivo* medical devices [37]. PDMS is a commonly used polymer for this application, as it is stable material, inert, and nontoxic, particularly when surrounded by body fluids.

PDMS inhibits organism attachment due to its surface properties and chemical composition. It is a non-polar material and is thus used extensively as a non-fouling surface due to its low modulus and surface energy. These characteristics encourage any organisms that attempt to cling to its surface to easily detach. The surface also resists protein absorption. In contrast, when polar polymers come in contact with living organisms, their protein molecules extensively absorb into surface to decrease the naturally high interfacial energy [38].

The surface stiffness of polymers can also be easily modified to meet desired specifications. PDMS is often patterned with micro- or nano- size features to control biofilm formation. It is hydrophobic, making it difficult for bacteria to adhere to its surface [39]. Natural anti-fouling surfaces such as shark skin or lotus leaves have similar properties to this polymer [40]. Its surface is often modified with topography to further increase the antifouling properties [1,5].

1.2.5 Approaches to Manufacturing Micro and Nano-features

Two general approaches were researched to texture the surfaces: top-down and bottom-up, as described in Table 1. The top down approach focused on methods that allow for control over the surface texture and geometry through physical means. Given the small scale of the features, there was a focus on mask-based photolithography and laser photolithography. The bottom-up approach looked at how particles could be added to the PDMS mixture itself to texture the surface. The main focus of this approach was coating particles followed by etching to leave behind a textured surface.

Method:	Mask-based photolithography mold	Molded pillars using laser photolithography	Printed pillars using laser photolithography coated in PDMS	Textured PDMS using ZnO particles, then etching particles
Approach type:	Top Down	Top Down	Top Down	Bottom Up
Feature size capabilities	~ 1 micron	~ 0.2 microns	~0.2 microns	50 nm – 5 microns (dependent on ZnO particles sizes)
Benefits:	1. Control over surface geometries and feature patterns 2. Saleable for mass manufacturing	1. More control over the surface texture, feature sizes and geometry 2. Scalable using methods such as roll to roll nanolithography	1. More control over surface texture, feature sizes and geometry 2. Method does not require as much process optimization	1. Easily feasible with available tools 2. Method well suited for mass manufacturing
Drawbacks:	1. Desired features sizes are beyond the lab machine capabilities	1. Pushing capability limits of Nanoscribe, resulting in prints varying from models.	1. Pushing capability limits of Nanoscribe, resulting in prints varying from models. 2. Unfeasible to mass manufacture and only used in a lab setting.	1. Less control over specific surface texture and geometry

Table 1: Approach Benefits and Drawbacks

Mask-based photolithography is comprised of creating a mask by fabricating a patterned surface unto a substrate, often called a wafer. The mask is then used to transfer the pattern to a photosensitive chemical photoresist on the substrate, followed by etching. Chemical treatments are then applied to enable the transfer of the pattern unto the material beneath the photoresist [41,42]. One of primary benefits of the mask-based photolithography its mass manufacturability. The method is widely used in the semiconductor industry and is therefore an established manufacturing process. Additionally, this method allows for control over the feature patterns, spacings, and geometry.

However, the desired feature sizes for this project are outside of the machine capabilities. Feature sizes are generally limited to approximately 1 micron or larger. For example, when used in the manufacturing process of semiconductors it is limited to patterning uncritical features [43]. This means that there are difficulties using this process to consistently manufacture submicron features. While there is significant control over surface pattern and geometry when within the machine capabilities, the desired feature size of 0.5 microns is slightly outside the 1-micron capability of the technology available.

One of the main benefits of laser photolithography compared to mask-based photolithography is that the machine capabilities better matched the desired feature sizes. The Nanoscribe GT+ can print lateral feature sizes down to 200 nm [44]. However, the desired 0.5 by 1-micron pillars are towards the end of

the capability limits. This could result in variation between the actual product compared to the program generated model. Another benefit is that the method is scalable. Though the Nanoscribe is limited to prints within a millimeter due to its ability to make extremely fine features, other similar methods could be used to mass manufacture a product with similar features [45]. For example, roll to roll imprint lithography can create features sizes down to approximately 300 nm, and can be used as a method to scale manufacturing [46].

Two different methods for laser photolithography were considered: molding pillars and directly printing pillars. In the first method, the mold would be created using laser photolithography and would then be used to shape the PDMS during the curing process, resulting in the textured surface [47, 45]. The second laser photolithography method involves printing the pillars directly and then coating the pillars in PDMS. The benefits are similar to the molding method in that feature sizes are within the Nanoscribe capabilities, allowing for better control over surface texture, features and geometries. Again, however, the desired features are at the capability limits, leading to differences from the actual prints compared to the models [48]. Another benefit is that this method does not require as much process optimization as the previous two methods. This is due to the fact that there is no molding or stamping involved. However, unlike the laser photolithography molding method, the procedure is not scalable for mass manufacturing. The Nanoscribe does not have the ability to print the pillars in a large volume, due to the limitations on the size of the print and time it takes to make each pillar [45]. Therefore, this technique is only feasible in a lab setting.

For the bottom-up approach, there was a focus on how ZnO particles could be added to the surface and then etched away, leaving behind textured PDMS. The benefits of this process are the ease of making the surface and the ability to easily mass produce the surface. However, this method does not provide much control over the surface texture, such as particle spacing or geometry. The only means of changing the texture with this method was to vary the concentration of ZnO particles on the surface and vary the size of the ZnO particles.

2.0 Objectives and Scope

There are two primary objectives for the project.

Objective 1. Test the hypothesis that combining material properties of high stiffness and surface features with size similar to that of *S. epidermidis* will result in a surface with reduced bacterial adhesion compared to that on surfaces having either property by itself. The experiments consist of two main parts: determining how stiffness affects bacterial adhesion and determining how stiffness and surface texture combined affect bacterial adhesion. Three different stiffnesses of PDMS are to be evaluated to determine how stiffness affects bacterial adhesion. Because PDMS is a hydrophobic material, it is expected that as the stiffness is increased, the substrate will more effectively prevent bacteria bio-fouling. The ideal stiffness will be used to create a textured surface.

Objective 2. Determine a scalable manufacturing method that can produce surfaces with specifically-designed micro- and nano- features. Both top-down photolithography approaches and bottom-up spin-coating approaches are to be investigated. The top-down approach uses a Nanoscribe 3-D printer to create a mold or directly print micropillars of sizes that are similar to that of *S. epidermidis*. The bottom-up approach involves mixing PDMS with each of three different zinc oxide particle sizes, then spin-coating the PDMS and etching the ZnO particles away to leave behind a porous textured PDMS.

These approaches will reduce bacterial adhesion due to the physicochemical forces at the contact surface. The bacteria cell count and percent area coverage are to be evaluated for the plain PDMS, as well as the textured surfaces. These results are to be compared to determine whether the combination of high stiffness and modified surface texture more effectively prevents bacterial adhesion than stiffness or surface texture by itself. The created surface will have the potential to reduce infections caused by biofilms in its application.

Due to lack of lab access during D-term 2020 due to the COVID-19 pandemic, fabrication of surfaces by bottom-up methods was not possible. Chapter 5 describes the experiments and analyses that would have been performed on bottom-up surfaces.

3.0 Methods

3.1 Fabrication of Anti-fouling Surfaces

The plain PDMS surfaces of varying stiffnesses were fabricated with different methods as shown in Figure 1, then analyzed. The textured surfaces with micropillars were first created with a mold, then as positive pillars. These were each coated with a thin layer of PDMS. The final set of modified substrates were spincoated with PDMS and ZnO particles of differing sizes. All surfaces were tested for *S. epidermidis* adhesion.
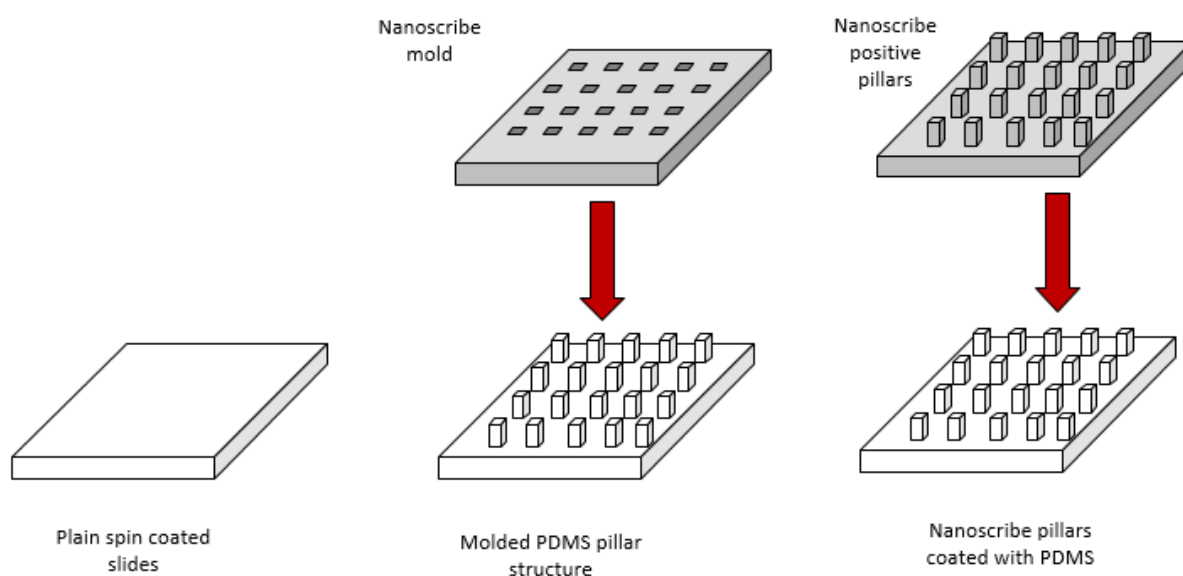
Figure 1: Surface Fabrication Methods

3.1.1 Control Surface Fabrication

The control surfaces were made as flat PDMS substrates of varying stiffnesses, using the method of O'Neill, Soo Hoo, and Walker [47]. Three samples of each stiffness were created and tested. These surfaces were prepared using SYLGARD184 Silicone Elastomer Kit (Dow Corning Corporation, Midland, MI). The stiffness was adjusted by varying the mass ratios of prepolymer to curing agent at 5:1, 20:1, and 40:1. The prepolymer and curing agent were thoroughly mixed at 200 rpm with a stir bar for 10 minutes to ensure the homogeneity of each mixture. The mixtures were then placed in a vacuum desiccator for 30 minutes to remove bubbles formed during mixing [46].

FTO glass pieces, approximately 2.5 x 2.5 cm, were cleaned in a sonicator with a 1:1:1 ratio of DI water to acetone to isopropyl alcohol and dried with nitrogen gas. A hotplate was set to 150ºC. The PDMS was spin coated onto the glass pieces at 500 rpm for 10 seconds, then 3000 rpm for 30 seconds. Once the hotplate was at 150ºC, the PDMS was cured for 10 minutes.

3.2 Stiffness Measurements

The samples were tested using the iMicro Pro nanoindenter system from Nanomechanics, Inc., a KLA-Tencor company. The standard Berkovich diamond indenter tip in the InForce 50 mN load was chosen instead of a flat-punch diamond indenter tip. While many reports in literature measuring polymeric materials make use of a flat-punch diamond indenter tip in order to apply a less severe strain field to the sample exposed to the compressive loads associated with indentation testing, the standard Berkovich diamond indenter tip that has become a stable of the instrumented indentation testing community due to its similarity comparability with a Vickers geometry.

The primary nanomechanical method used to study the samples was the "Advanced Dynamic E and H" option that operates with a constant strain rate during the application of load onto the specimen during testing. The testing protocol is classified as a continuous stiffness measurement and therefore enables stiffness and additional properties to be measured as a function of depth into the sample, rather than conventional static indentation testing which can only measure the sample stiffness as the indenter begins to unload.

When the "Advanced Dynamic E and H" method was used the maximum depth that was reached during testing was set at approximately 1000 nm in order to keep with some of the earlier work reported on indentation testing of PDMS [49]. An initial test yielded Elastic Modulus values greater than 100 MPa. This is well above the reported values of 1.00 to 9.99 MPa found in literature [50-53]. It was assumed the thin-film effect was potentially influencing the recorded values since the PDMS surfaces were spin-coated onto glass slides that are known to have an elastic modulus of 72,000 MPa. Therefore, in order to address this effect, the "Dynamic CSR for Thin Films" method was used to provide the stiffness results.

3.3. Top-Down Fabrication of Anti-Fouling Surfaces

3.3.1 Pillar Structure

A PDMS surface was designed with nine varying topographies, containing three different topographical shapes and three different spacings. The topographies were as follows: square pillars, square pillars with rounded edges (100 nm fillet), and square "domed" pillars (100 nm fillet on both edges). All pillars were 1 μm in height. The square and domed pillars were both 0.5 μm in width, while the circular pillar was 0.5 μm in diameter. Each pillar type was designed with three different spacings: 425, 600, and 1500 nm. The three proposed pillar shapes are shown below in Figure 2.
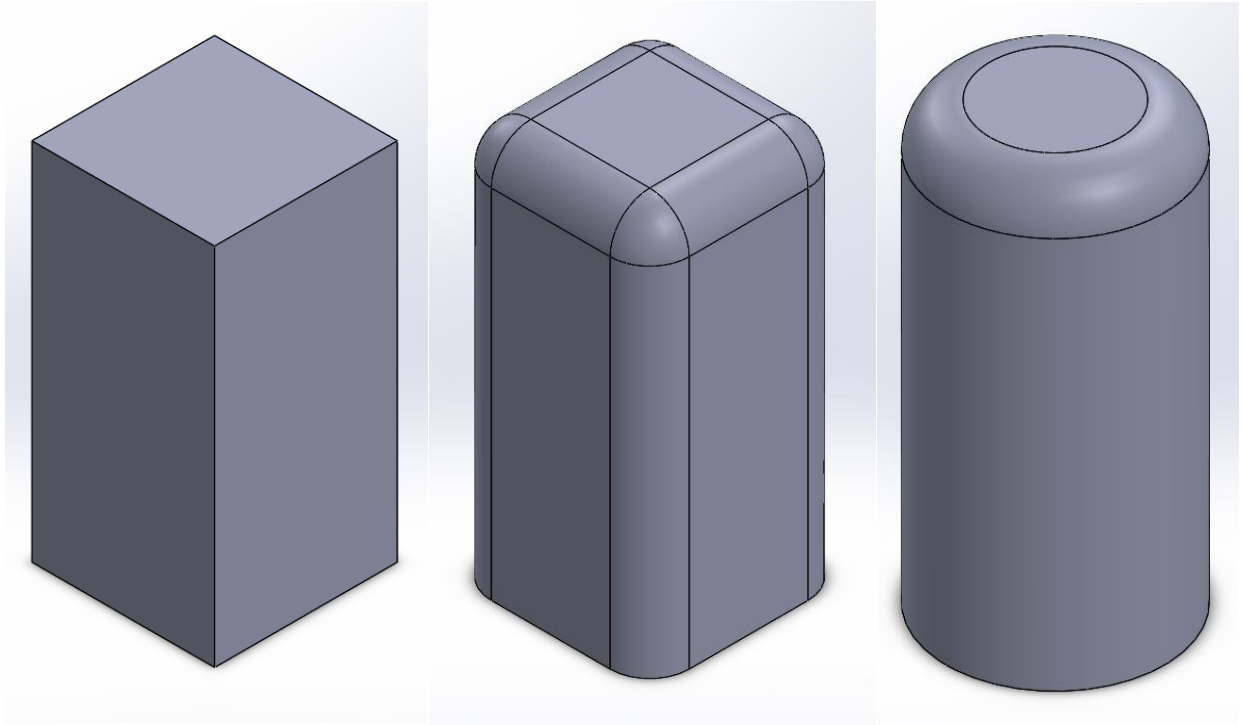
Figure 2: Square, Domed and Circular Micropillar Proposed Images

In order to increase the speed of testing with so many different variables, the varying pillars and spacings were composed into a 3x3 grid shown below in Figure 3.

Square 425 nm	Circular 1500 nm	Domed 600 nm
Domed 1500 nm	Square 600 nm	Circular 425 nm
Circular 600 nm	Domed 425 nm	Square 1600 nm

Figure 3: Pillar Layout

3.3.2 Molded Pillars

The first method involved creating a mold by two photon lithography using the Nanoscribe Photonic Professional GT+ with IP-Dip resin. The Nanoscribe Photonic Professional GT is a three-dimensional printer that utilizes two photon polymerization. This is a technique that uses high intensity lasers to create complex three-dimensional structures. The process involves photosensitive materials, known as photoresists, a precise positioning stage, and the computer program that controls the procedure. Two photon polymerization occurs when lasers create femtosecond pulses that cause the photoresists to absorb photons. Following the printing process, excess photoresist material is washed off to uncover the structure [47].

The Nanoscribe has features that allow for precise customization. It has the ability to print lateral feature sizes down to 200 nm. The finest vertical resolution is specified as 1500 nm [44]. Two types of photoresist were considered: IP-Dip and IP-S. IP-Dip is an acrylate ideal for submicron features and high aspect ratios. IP-S is a methacrylate that is ideal for smooth surfaces of micron and mesoscale fabrication [54]. IP-Dip was chosen due to the minute size of the pillars. A complete list of the photoresist properties can be found in Appendix A.

This mold contained holes of varying shapes and spacings that was used to create arrays of pillars on a PDMS surface. The mold was created with arrays of different blocks of varying widths and hole types (Figure 3 and 4). To change the spacings between 425, 600 and 1500 nm, the block widths varied in order to match the appropriate sizes: 925, 1100 and 2000 nm, respectively. These can be seen in Figures 4 and 5 below. The hole size and block height remain the same, but the block width changed to achieve the desired spacing.
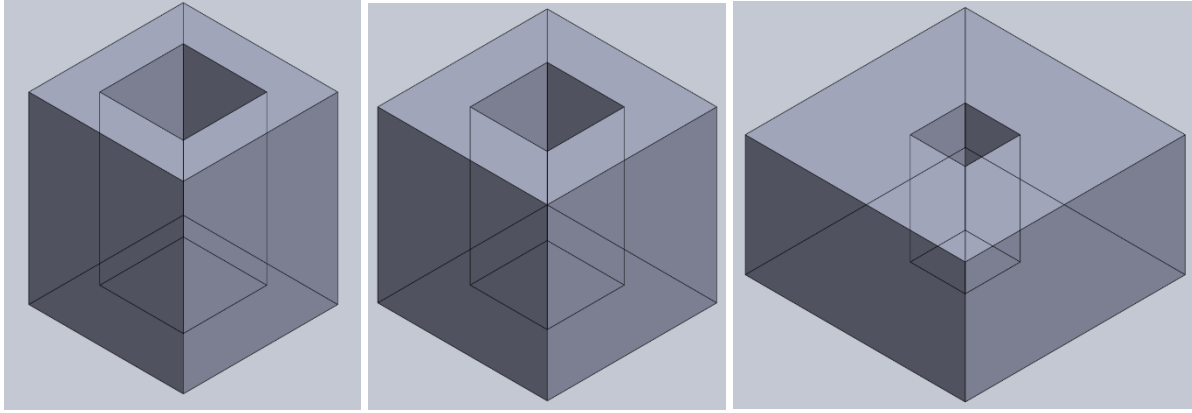
Figure 4: Block Width Variation
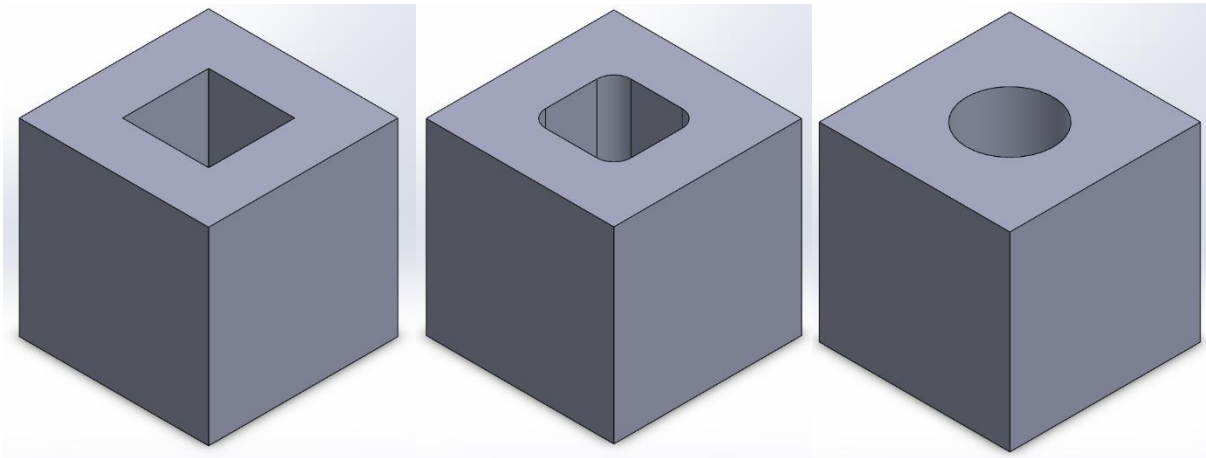
Figure 5: Square, Domed and Circular Mold Structures for 600 nm Spacing

A mold with the negative of the surface patterns described above was generated using the Nanoscribe two photon lithography by patterning a thin layer of IP-Dip onto a glass slide [47]. The slide was placed in isopropyl alcohol (IPA) for 20 minutes, followed by acetone for 5 minutes, in order to cure the IP-Dip onto the surface.

The glass slide with the negative mold pattern was placed flat on the bottom of an aluminum dish. The PDMS was prepared using SYLGARD184 Silicone Elastomer Kit. The stiffness was adjusted by varying the mass ratios of prepolymer to curing agent at 5:1, 20:1, and 40:1 to attain stiffnesses of 0.1, 1.0, and 2.6 MPa, respectively. The prepolymer and curing agent were thoroughly mixed with a stir bar for 15

minutes at 200 rpm to ensure the homogeneity of each mixture [46,47]. The mixtures were then placed in a vacuum desiccator for 30 minutes to remove bubbles formed during mixing [55].

A foil dish for each mold was placed on a hotplate at room temperature. Then, each degassed PDMS mixture was carefully poured into the mold in the the foil dishes. The hotplate was set to 150ºC. Once at 150ºC, the PDMS was cured for 10 minutes. The foil dishes were removed from the hot plate and allowed to cool at room temperature [47]. The PDMS surfaces were then carefully peeled away from the molds and stored in a petri dish.

3.3.3 Positive Pillars

The second method involved printing the positive pillar structures directly onto a glass slide using the Nanoscribe two photon lithography. Although this method is much less scalable than using two-photon lithography to create a master mold or stamp, it involves fewer steps and has a higher likelihood of success as an initial demonstration of feasibility The printed pillars were cured following the same procedure as above: 20 minutes in IPA, followed by 5 minutes in acetone. The slide was then immediately placed into a clean petri dish and covered to prevent other particles from coating the surface and texturing the PDMS coating.

The PDMS was prepared using SYLGARD184 Silicone Elastomer Kit. Toluene was also added to the mixture in order to dilute the PDMS for spin coating, using a 1:10 ratio of toluene to PDMS. The prepolymer, curing agent and toluene were thoroughly mixed with a stir bar for 30 minutes at 200 rpm to ensure the homogeneity of the mixture. The mixture was then placed in a vacuum desiccator for 30 minutes to remove bubbles formed during mixing. The mixture was spin coated at 3000 rpm for 50 seconds over the glass slide with the Nanoscribe pillars.

3.4. Bottom-Up Fabrication of Anti-Fouling Surfaces

3.4.1 Microparticle Textured Surface

Three samples of each ZnO particle size were created and tested. The PDMS was first prepared using SYLGARD184 Silicone Elastomer Kit. The stiffness was adjusted by varying the mass ratio of prepolymer to curing agent at the ratio that created the stiffness with the least bacterial adhesion, based on previous testing.

Sigma-Aldrich ZnO nanopowder of <50 nm, 200 nm, and 5 µm particle sizes were added to the PDMS mixture in a mass ratio of 1:2, each particle size mixture in a separate vial. The prepolymer, curing agent, and ZnO particles were thoroughly mixed at 400 rpm with a stir bar for 20 minutes to ensure the homogeneity of each mixture. The mixtures were then placed in a vacuum desiccator for 30 minutes to remove bubbles formed during mixing.

FTO glass pieces, approximately 2.5 x 2.5 cm, were cleaned in a sonicator with a 1:1:1 ratio of DI water to acetone to isopropyl alcohol and dried with nitrogen gas. A hotplate was set to 150ºC. The PDMS and ZnO mixture were spin coated onto the glass pieces at 500 rpm for 10 seconds, then 3000 rpm for 30 seconds. Once the hotplate was at 150ºC, the PDMS was cured for 10 minutes.

The glass pieces with the PDMS and ZnO particles were placed in a petri dish filled with 5% hydrochloric acid to etch out the ZnO particles. The pieces were left in the dish overnight or until the particles were etched out, as shown by when the surface of the glass pieces was slightly opaque, as opposed to white when initially spin coated. The process is shown in Figure 6.
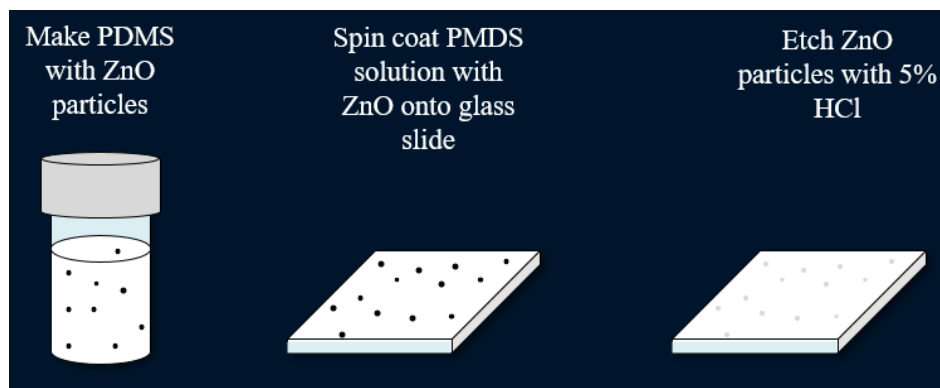
Figure 6: PDMS Texturing with ZnO Process

The three different sizes of the ZnO particles were also analyzed and verified by spincoating ZnO by itself onto glass slides. These were then imaged with the SEM.

3.5 Bacterial Testing of Anti-fouling Surfaces

3.5.1 Bacterial Strains

The liquid culture was prepared using 10-12 mL of TSB glucose solution and placed in an incubator overnight, while shaking at 200 rpm. The bacteria concentration was diluted to 5×10^5 CFU/mL [56,57]. Step by step instruction for the bacteria procedure can be found in Appendix A.

3.5.2 Measurements of Bacterial Attachment and Biofilm Formation

The surface being was sterilized by soaking in 70% ethanol for 10 minutes. It was rinsed three times with sterile water using a serological pipette and placed on the bottom of a six-well plate. A micropipette was used to add the bacteria culture that had a concentration of 5×105 CFU/ml to the well so that the PDMS surface was submerged, about 0.75 mL. The well plate was incubated while shaking at 60 rpm for 5 hours in the first round of testing, 18 hours in the second round, and 24 hours in the third round of testing.

The surface was taken out of the well with the bacteria suspension and placed in an empty well plate. About 5 mL of media was added and tweezers were used to move the surface around within the well plate while keeping it submerged for 30 seconds. The bottom of the surface was wiped dry with a paper towel and the surface was placed on a glass slide. A micropipette was used to add 0.5 µL of a solution of SYTO 9 at a concentration of 5 mM in DMSO to 50 µL of media in a centrifuge tube and combined using the micropipette. Less than 5 µL of the solution was micro pipetted on the center of the PDMS surface. The surface was incubated for 5 minutes to allow the stain to absorb into the bacterial cells. A coverslip was placed on the surface.

A Leica DM LB2 fluorescence microscope was used to image three areas on the sample at 40x magnification. The cell count on each type of topography was compared using data obtained from ImageJ [57].

After converting the TIFF files to 8-bit images, the threshold values were adjusted until the adjusted images best matched the original images. An example of the process is shown in Figure 7 below. The cell count feature was then used to analyze the number of cells, total area and % area covered.
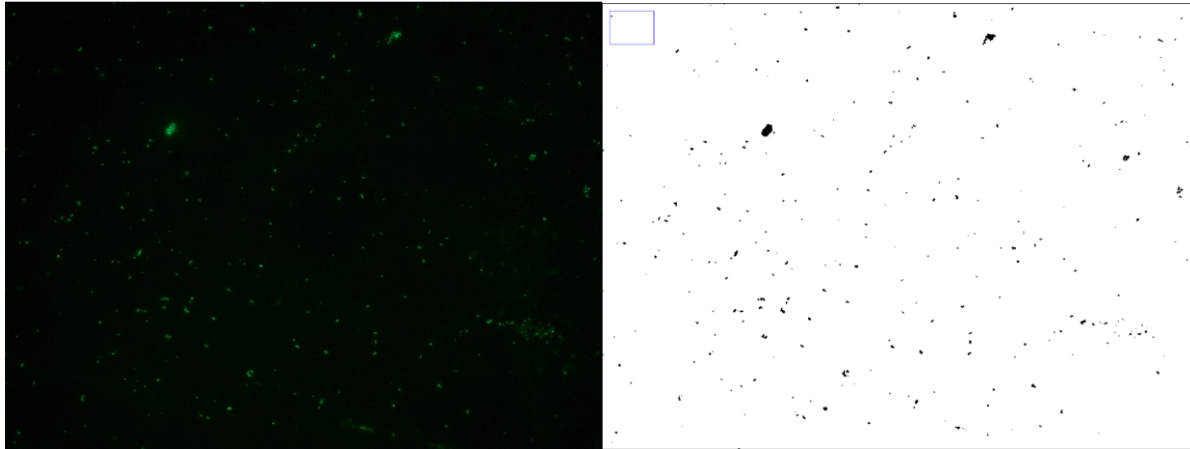
Figure 7: Comparison of Original Fluorescence Image and Adjusted ImageJ File

4.0 Results and Discussion

4.1 Results on Control surface

The PDMS slides were first analyzed using a Nano indenter to measure stiffness. The slides were then tested for bacterial adhesion. Different samples were tested for different times to find the testing time that provided the most standard results across the varying stiffnesses. The results partly correlated with prior research.

4.1.1 PDMS Stiffness Decreased as the Cross-Linking Decreased

The average stiffnesses for the 5:1, 20:1 and 40:1 PDMS ratios are 331.5, 328.5 and 228 N/m respectively. The summary results are shown in Table 2 below. Test results for each individual cycle can be found in Appendix C. It is interesting to note how there is little variation between stiffness for the 5:1 PDMS and the 20:1 PDMS. It is possible that sample 1 is an outlier due to the fact that the stiffness values better correlate to the 40:1 results. Another test on the 5:1 sample would need to be done to confirm.

One other thing to note is the variance within a single sample, as can be seen with the large standard deviation values. This could possibly explain some of the bacteria adhesion results in which some sections within a sample would saw significant biofilm growth, while others saw little growth.

	5:1 PDMS Stiffness (N/m)	St. Dev.	20:1 PDMS Stiffness (N/m)	St. Dev.	40:1 PDMS Stiffness (N/m)	St. Dev.
Sample 1	227	81.2	306	81.4	227	81.2
Sample 2	436	171	351	67.4	229	81.7
Average	**331.5**	**126.1**	**328.5**	**74.4**	**228**	**81.45**

Table 2: Stiffness Results

4.1.2 Materials with Decreasing Stiffness Revealed Less Bacterial Growth

In the first round of testing, *S. epidermidis* was grown for approximately five hours to test initial bacteria adhesion to the surfaces. The average cell counts are shown in Table 3 below. Test results for each individual round can be found in Appendix D. Surprisingly, the results show the opposite of what was expected, as the cell count, total area, and percent area averages decrease with decreasing stiffness instead of increase with decreasing stiffness, as previous research has shown [5,32]. As can be seen in Figures 8-10, the number of bacteria cells, as shown by the green dots, becomes less as the ratio of PDMS decreases.

Sample Type	Cell Count Average	Standard Deviation	Average Total Area	Standard Deviation	Average % Area	Standard Deviation
5:1 (high stiffness)	314	21.4	0.148333	0.01	0.272333	0.02
20:1 (medium stiffness)	105.3333	68.7	0.088	0.05	0.161667	0.10
40:1 (low stiffness)	33	6.9	0.020667	0.01	0.037667	0.02

Table 3: Initial Bacteria Testing Results
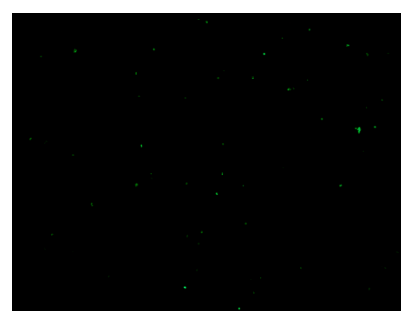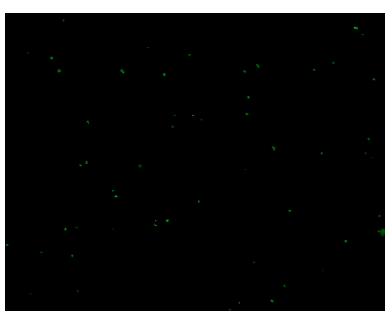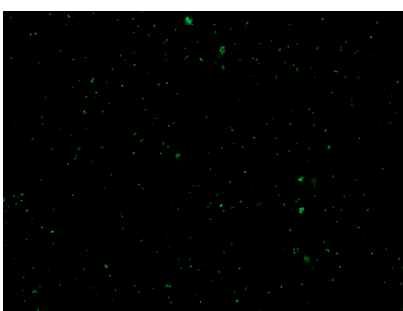
Figure 8: 5:1 PDMS Bacteria Growth *Figure 9: 20:1 PDMS Bacteria Growth* *Figure 10: 40:1 PDMS Bacteria Growth*

4.1.3 Longer Testing Shows That Moderate Stiffness Yields Best Results

Two more tests were conducted for a longer time period in order to look at biofilm growth on the surfaces. *S. epidermidis* was grown on the 5:1 PDMS samples for 18 hours, whereas on the 20:1 and 40:1 samples, the bacteria was grown for 24 hours. The average cell counts are shown in Table 4 below. Test results for each individual round can be found in Appendix D. The results show that bacteria growth was significantly less on the 5:1 samples, as compared to both the 20:1 and 40:1 samples.

Sample Type	Cell Count Average	Standard Deviation	Average Total Area	Standard Deviation	Average % Area	Standard Deviation
5:1 Sample 2 and 3 Averages	265	199	0.859	2.07	1.573	3.79
20:1 Sample 2 and 3 Averages	2822	1374	12.224	15.01	22.384	27.49
40:1 Sample 2 and 3 Averages	2605	1445	9.587	6.76	17.554	12.38

Table 4: Subsequent Bacteria Testing Results

There are, however, several factors that lead to inconclusive results. The first was that samples 2 and 3 of the 5:1 PDMS were grown for less time than the latter two samples of 20:1 and 40:1 PDMS, which makes them difficult to compare. Furthermore, the 5:1 PDMS samples primarily had groupings of bacteria, shown in Figures 11-13, as opposed to homogeneity, as was seen in the samples from the first round of testing.
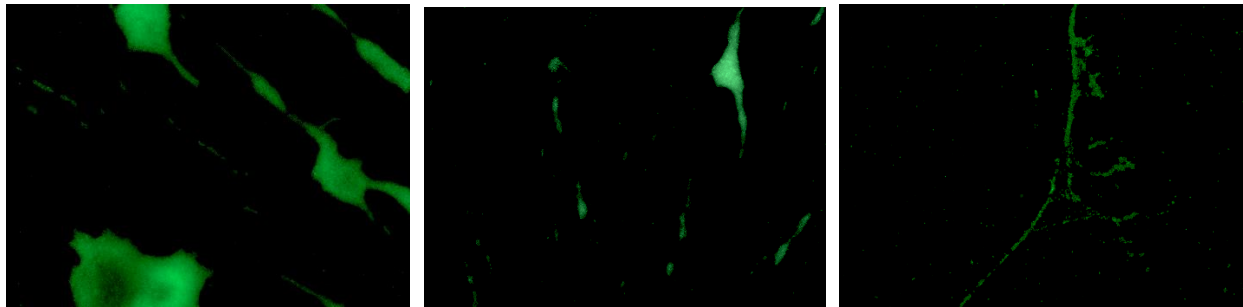
Figure 11: 5:1 PDMS Sample 2 Image 1   *Figure 12: 5:1 PDMS Sample 2 Image 2*   *Figure 13: 5:1 PDMS Sample 3 Image 1*

Another major problem was that during testing, the bacteria growing in the well plates and on the bottom of the samples would detach and then reattach to the samples during the growth period. This can be seen in some of the images of the 20:1 and 40:1 samples, shown in Figures 14-16, where the bacteria seemed to be out of focus and covered in other layers of growth. The difficulty in focusing the images likely resulted from the bacteria growing on different planes.
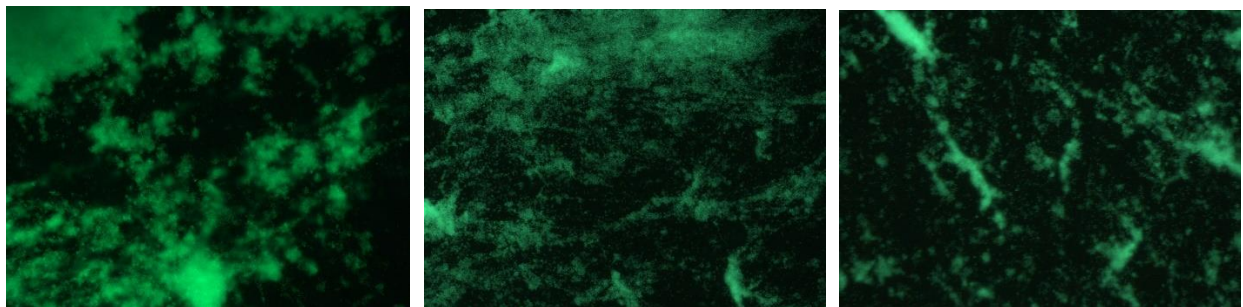
Figure 14: 20:1 PDMS Sample 2 Image 3   *Figure 15: 20:1 PDMS Sample 3 Image 1*   *Figure 16: 40:1 PDMS Sample 3 Image 1*

Furthermore, the results still do not match the previous research given the fact that the 20:1 samples had more bacterial adhesion than the 40:1 samples, as shown in Figures 17 and 18. Again, this could possibly be because the bacteria detached from the well plate or bottom of the slide and then reattached to the surface.

24
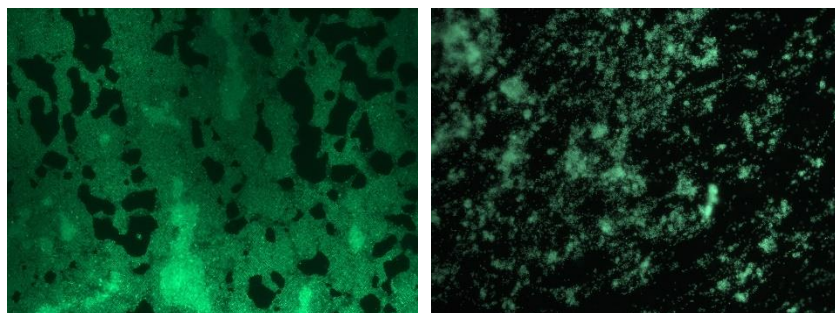
Figure 17: 20:1 PDMS Sample 3 Image 2   Figure 18: 40:1 PDMS Sample 3 Image 2

It is also possible that stiffness variations within a sample surface could account for some of the heterogeneity in biofilm growth between sections of the sample. Since many of the cells in the images developed clusters, the cell count is not as accurate, so the comparisons of the results are based on total area and percent area.

The team had planned on completing more testing over a shorter growth interval in order to come to a better understanding of the effect of stiffness. Without this testing it is difficult to draw any significant conclusions.

4.2 Results on Top-Down Surfaces

Both methods of micropillar fabrication, molded pillars and positive printed pillars, were attempted. Neither provided the desired results, and so different surface modifications were subsequently used.

4.2.1 Molded Pillars

The SEM image of the pillar mold array is shown in Figure 19. Several problems arose which prevented the group from pursuing this idea further. One of the major issues was that the PDMS stuck to the IP-Dip Resin mold. When the PDMS was removed from the glass slide on which the Nanoscribe mold was printed, the mold stuck to the PDMS and was ripped off the glass slide.
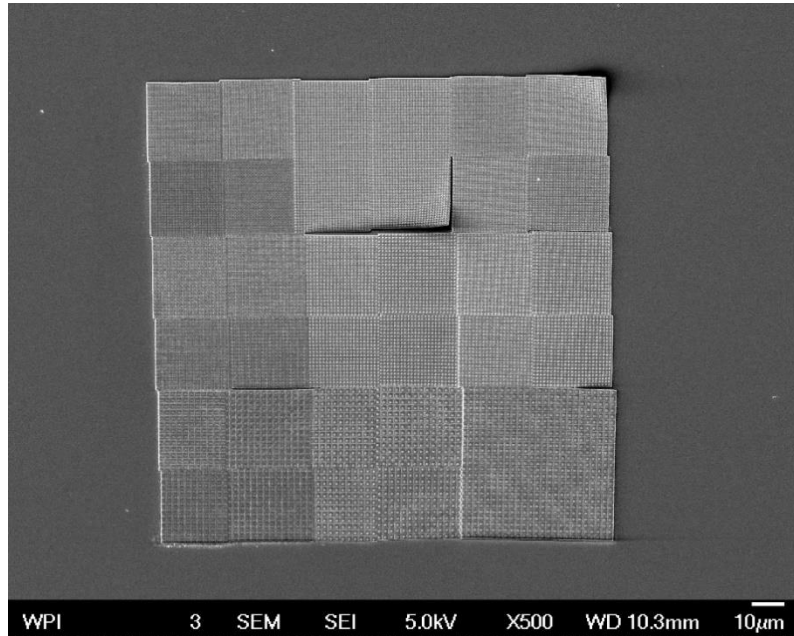
Figure 19: SEM Image of Nanoscribe Pillar Stamp Array

Furthermore, the pillar structures and molds proposed were at the limits of the capabilities for the Nanoscribe. As a result, the Nanoscribe mold greatly varied from the computer model. Based on SEM images, the holes in the printed mold were significantly smaller, with a diameter of approximately 250 nm, as opposed to the specified 500 nm diameter. In some cases, the holes were completely filled in, as shown in Figure 20.
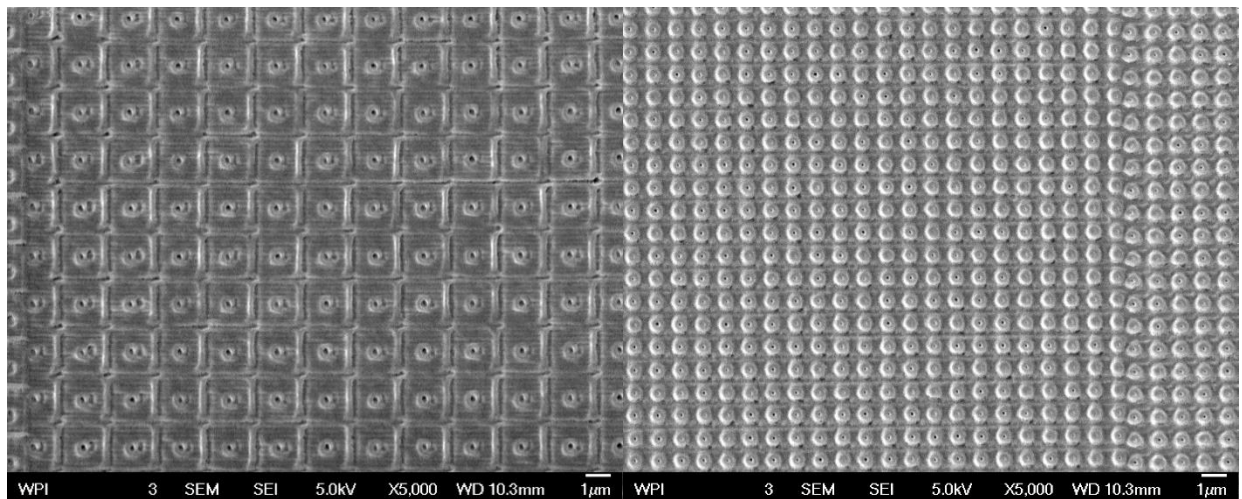
Figure 20: Surface Contained Undesired Variations and Filled in Holes

Another issue was that the Nanoscribe left outlined squares around each pillar hole, which would have affected the PDMS structure when molded. In another part of the array, one of the sections curled up at the corner, as shown below in Figure 21. All four of these problems lead to the decision to attempt another process rather than using a mold with the PDMS.
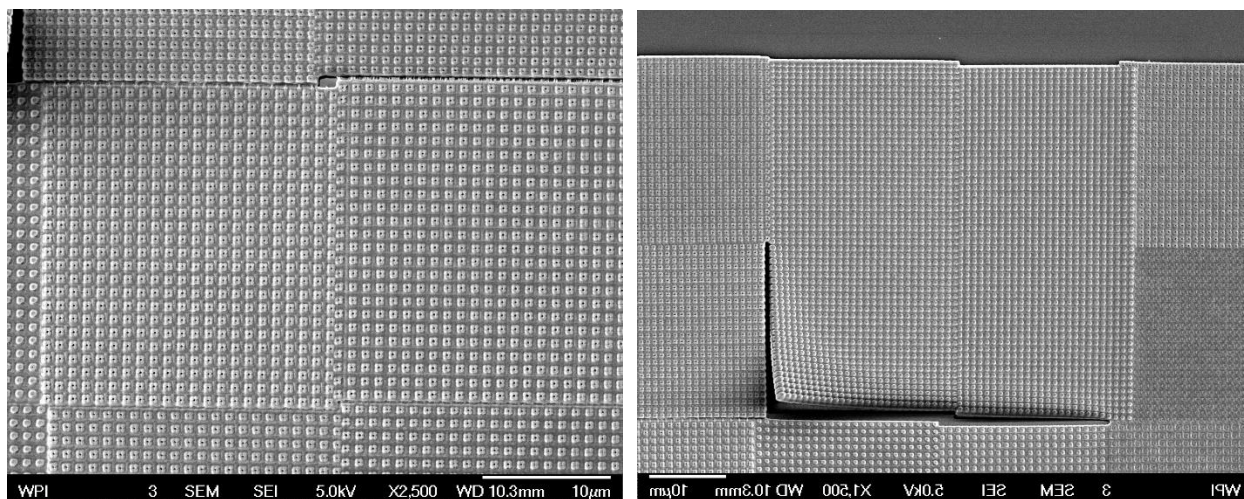
Figure 21: Sections Did Not Line Up Correctly

4.2.2 Positive Pillars

The positive pillars also had problems which inhibited the group from using them to test the hypothesis. The pillars were printed and spin coated with PDMS. However, when the sample was imaged with the SEM, there was no sign of the pillars or the printed triangle used to mark the pillar locations on the glass slide. It was hypthesized that the use of toluene to dilute the PDMS solution may have dissolved the IP-Dip, that the PDMS coating was too thick and completely covered the pillars, or that the spincoating process damaged the pillars.

Since the design was at the capability limits of the Nanoscribe, it is likely that several tests would still need to be done to determine the proper print speed and laser power settings. Because many of the holes in the mold array were much smaller than specified, pillar dimensions would need modifications to meet the original design and to account for the PDMS coating. Additionally, as shown below in the Describe software simulated images of the pillars in Figure 22, there is little difference between the domed pillars and square pillars. Given the minute size of the pillars, it is likely that it is not possible to create such small features with the Nanoscribe.
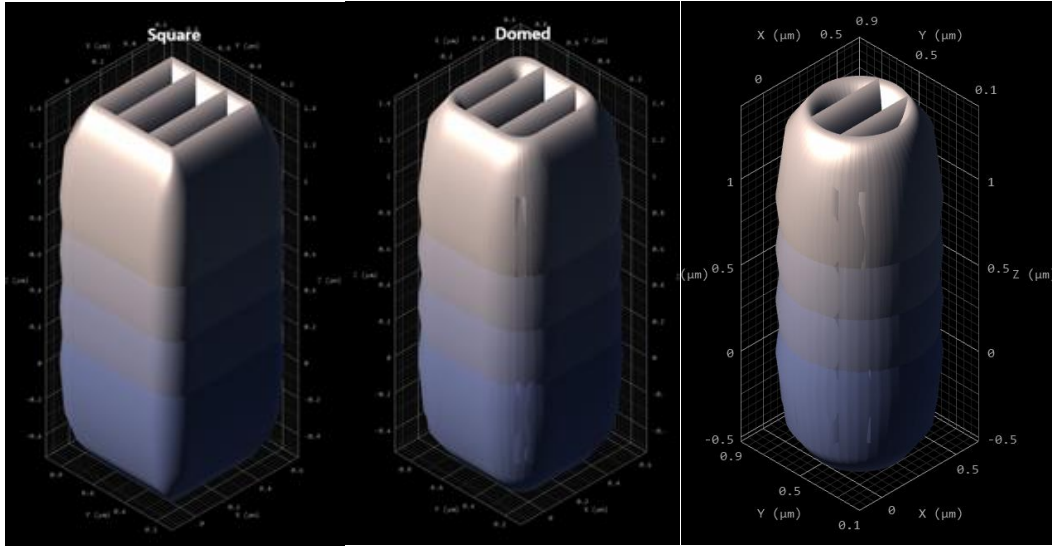
Figure 22: Square, Domed and Circular Micropillar Describe Simulated Images

Due to the time constraints of the MQP, both methods were decided against in favor of developing a new type of surface that would allow for bacteria adhesion tests to be completed within the given timeframe. The transition to the bottom-up approach was planned for D term, but due to lack of lab access due to the COVID-19 pandemic during this time, bottom-up surfaces were not investigated.

4.3 Anticipated Results on Bottom-Up Surfaces

Based on previous research that studies how substrate stiffness affects bacterial adhesion, the 5:1 PDMS ratio was expected to have the most effective antifouling properties due to low stiffness, its non-polar and low surface energy characteristics [5,32]. Furthermore, the 200 nm ZnO particles would be the most effective of the three particles sizes. This diameter is smaller than that of *S. epidermidis* and thus would decrease adhesion to the substrate due to the physicochemical forces at the surface [18,19]. Therefore, the combination of etched 200 nm ZnO particles and 5:1 PDMS would theoretically yield better results than either by itself.

4.3.1 Interpretation of Results

The experimental results would be analyzed in the following way. The bacteria count and area coverage averages would be compared between the etched slides with the three different types of ZnO particles. Based on which particle had the least bacterial adhesion, the results would be compared with that of the plain spin coated slide of the same stiffness. A statistical analysis between these two types of slides would be compared to determine if the results are significant.

4.3.2 Comparison to Hypothesis

The results would be used to inform the conclusions and accept or reject the initial hypothesis. The results would be significant if the slides with the etched ZnO particles and the most effective antifouling PDMS ratio prevented bacterial adhesion better than the PDMS by itself. If this was the case, then further research would need to be done to determine if this is a potential solution to biofilm adhesion.

If the results from the combination of PDMS stiffness and etched ZnO particles lead to more bacterial adhesion than just the flat PDMS surfaces, it might lead to the conclusion that stiffness and texture do not interact in a way that more effectively prevents bacteria biofouling. More research, however, would need to be done to confirm this conclusion.

6.0 Conclusion: Findings and Recommendations

Three varying stiffness of PDMS were developed and tested for adhesion of *S. epidermidis.* The results were varied, though some correlated with prior research and anticipated outcomes. During the 5 hour initial adhesion tests, results revealed that adhesion decreased with decreasing stiffness. However, in the 18-24 hour bacteria growth trials which tested biofilm growth, the results were contrary. There was some evidence that increased stiffness reduced bacteria adhesion, however this could be due to shorter growth times than the other surfaces.

Fabrication of top-down surfaces was investigated by using two-photon photolithography printing of a mold and by direct printing of features. The results showed that this fabrication method does not have sufficient resolution to print features at sizes small enough to match the size of *S. epidermidis*, which is 0.5 microns. Furthermore, due to lack of lab access during D-term 2020 due to the COVID-19 pandemic, bottom-up surfaces were not investigated. However, it is anticipated that the bottom-up synthesis would have provided surfaces with texture having size similar to and smaller than that of *S. epidermidis*.

Finally, testing was done on the influence of stiffness on the adhesion and growth of *S. epidermidis*, but the combination of stiffness and surface texturing was not tested. Ultimately, more testing needs to be done to determine how stiffness affects *S. epidermidis* adhesion to PDMS and whether combining the characteristics of stiffness and surface texture could further reduce bacteria adhesion. Due to the lack of testing, the group hopes that more research can be done to either support or disprove the hypothesis that combing the properties of high stiffness and surface texture will reduce biofilm formation more than either characteristic by itself. The group recommends the use of scalable bottom-up PDMS/ZnO method for generating textured surfaces in future work. If this surface design was effective, it could be beneficial for *in vivo* devices because it does not involve any potentially harmful chemicals or metals.

7.0 References

[1] Wang, B.; Ye, Z.; Tang, Y.; Han, Y.; Lin, Q.; Liu, H.; Chen, H.; Nan, K. Fabrication of nonfouling, bactericidal, and bacteria corpse release multifunctional surface through surface-initiated RAFT polymerization. International journal of nanomedicine 2017, 12, 111-125

[2] Renner, L. D.; Weibel, D. B. Physicochemical regulation of biofilm formation. MRS Bulletin 2011, 36, 347-355.

[3] J.D. Bryers , Biotechnology Bioengineering. 100 (1), 1 (2008).

[4] Keith D. Lind; JD; MS AARP Public Policy Institute. Understanding the Market for Implantable Medical Devices.

[5] Li M, Neoh KG, Xu LQ, et al. Surface modification of silicone for biomedical applications requiring long-term antibacterial, antifouling, and hemocompatible properties. Langmuir. 2012;28(47):16408–16422.

[6] Costerton JW, Stewart PS, Greenberg EP. Bacterial biofilms: a common cause of persistent infections. Science. 1999;284(5418):1318–1322.

[7] A.G. Gristina , Science 237 (4822), 1588 (1987).

[8] B.V. Derjaguin , L. Landau , Actual Physical Chim. 14 , 633 (1941).

[9] Banerjee, I.; Pangule, R. C.; Kane, R. S. Antifouling Coatings: Recent Developments in the Design of Surfaces That Prevent Fouling by Proteins, Bacteria, and Marine Organisms. Advanced Materials 2011, 23, 690-718.

[10] K. D. Park, Y. S. Kim, D. K. Han, Y. H. Kim, E. H. B. Lee, H. Suh, K. S. Choi, Biomaterials 1998, 19, 851.

[11] P. Chaignon, I. Sadovskaya, C. Ragunah, N. Ramasubbu, J. B. Kaplan, S. Jabbouri, Appl. Microbiol. Biotechnol. 2007, 75, 125.

[12] Widerström, M. Significance of Staphylococcus epidermidis in Health Care-Associated Infections, from Contaminant to Clinically Relevant Pathogen: This Is a Wake-Up Call. Journal of clinical microbiology 2016, 54, 1679-1681.

[13] Otto M. 2009. Staphylococcus epidermidis–the 'accidental' pathogen. Nat Rev Microbiol 7:555–567. doi:10.1038/nrmicro2182.

[14] Kahl BC, Becker K, Loffler B. 2016. Clinical significance and pathogenesis of staphylococcal small colony variants in persistent infections. Clin Microbiol Rev 29:401–427. doi:10.1128/CMR.00069-15.

[15] Becker K, Heilmann C, Peters G. 2014. Coagulase-negative staphylococci. Clin Microbiol Rev 27:870–926.

[16] Archer GL. 1988. Molecular epidemiology of multiresistant Staphylococcus epidermidis. J Antimicrob Chemother 21(Suppl C):133–138. doi:10.1093/jac/21.suppl_C.133.

[17] Dahl V, Tegnell A, Wallensten A. 2015. Communicable diseases prioritized according to their public health relevance, Sweden, 2013. PLoS One 10:e0136353. doi:10.1371/journal.pone.0136353.

[18] Tripathy, A.; Sen, P.; Su, B.; Briscoe, W. H. Natural and bioinspired nanostructured bactericidal surfaces. Advances in Colloid and Interface Science 2017, 248, 85-104.

[19] Ghilini, F.; Pissinis, D. E.; Miñán, A.; Schilardi, P. L.; Diaz, C. How Functionalized Surfaces Can Inhibit Bacterial Adhesion and Viability. ACS Biomaterials Science & Engineering 2019, 5, 4920-4936.

[20] Ghilini, F.; Pissinis, D. E.; Miñán, A.; Schilardi, P. L.; Diaz, C. How Functionalized Surfaces Can Inhibit Bacterial Adhesion and Viability. ACS Biomaterials Science & Engineering 2019, 5, 4920-4936.

[21] Chung, K.; Schumacher, J.; Sampson, E.; Burne, R.; Antonelli, P.; Brennan, A. Impact of engineered surface microtopography on biofilm formation of Staphylococcus aureus. Biointerphases 2007, 2, 89-94.

[22] Ronn S. Friedlander; Hera Vlamakis; Philseok Kim; Mughees Khan; Roberto Kolter; Joanna Aizenberg Bacterial flagella explore microscale hummocks and hollows to increase adhesion. Proceedings of the National Academy of Sciences of the United States of America 2013, 110, 5624-5629.

[23] Hochbaum, A. I.; Aizenberg, J. Bacteria Pattern Spontaneously on Periodic

Nanostructure Arrays. Nano Letters 2010, 10, 3717-3721.

[24] Tripathy, A.; Sen, P.; Su, B.; Briscoe, W. H. Natural and bioinspired nanostructured bactericidal surfaces. Advances in Colloid and Interface Science 2017, 248, 85-104.

[25] D. Lee, R. E. Cohen, M. F. Rubner, Langmuir 2005, 21, 9651.

[26] J. Sawai, H. Igarashi, A. Hashimoto, T. Kokugan, M. Shimizu, J. Chem. Eng. Jpn. 1995, 28, 288.

[27] L. L. Zhang, Y. H. Jiang, Y. L. Ding, M. Povey, D. York, J. Nanopart. Res. 2007, 9, 479.

[28] H. J. Lee, S. Y. Yeo, S. H. Jeong, J. Mater. Sci. 2003, 38, 2199.

[29] A. M. Derfus, W. C. W. Chan, S. N. Bhatia, Nano Lett. 2004, 4, 11.

[30] J. C. K. Lai, M. B. Lai, S. Jandhyam, V. V. Dukhande, A. Bhushan, C. K. Daniels, S. W. Leung, Int. J. Nanomed. 2008, 3, 533.

[31] S. J. Cho, D. Maysinger, M. Jain, B. Roder, S. Hackbarth, F. M. Winnik, Langmuir 2007, 23, 1974.

[32] Kolewe, K. W.; Peyton, S. R.; Schiffman, J. D. Fewer Bacteria Adhere to Softer Hydrogels. ACS applied materials & interfaces 2015, 7, 19562-19569.

[33] Saha, N.; Monge, C.; Dulong, V.; Picart, C.; Glinel, K. Influence of polyelectrolyte film stiffness on bacterial growth Biomacromolecules 2013, 14, 520– 528

[34] Song, F.; Ren D. Stiffness of Cross-Linked Poly(Dimethylsiloxane) Affects Bacterial Adhesion and Antibiotic Susceptibility of Attached Cells. 2014.

[35] Lichter, J. A.; Thompson, M. T.; Delgadillo, M.; Nishikawa, T.; Rubner, M. F.; Van Vliet, K. J. Substrata mechanical stiffness can regulate adhesion of viable bacteria Biomacromolecules 2008, 9, 1571– 1578

[36] Kolewe, K. W.; Zhu, J.; Mako, N. R.; Nonnenmann, S. S.; Schiffman, J. D. Bacterial Adhesion Is Affected by the Thickness and Stiffness of Poly(ethylene glycol) Hydrogels. ACS applied materials & interfaces 2018, 10, 2275-2281.

[37] Y. D. Kim, J. S. Dordick, D. S. Clark, Biotechnol. Bioeng. 2001, 72, 475.

[38] S. Krishnan, C. J. Weinman, C. K. Ober, J. Mater. Chem. 2008, 18, 3405.

[39] H. M. Shang, Y. Wang, S. J. Limmer, T. P. Chou, K. Takahashi, G. Z. Cao, Thin Solid Films 2005, 472, 37.

[40] Scardino A J, Hudleston D, Peng Z, Paul N A and de Nys R 2009 Biomimetic characterisation of key surface parameters for the development of fouling resistant materials Biofouling 25 83–93

[41] Hermatschweiler, Martin and Thiel, Michael. Three-dimensional laser lithography. Wiley-VCH Verlag GmbH & Co. KGaA, Weinheim. 2011

[42] R. A. Cirellia, G. P. Watson, O. Nalamasuc. Optical Lithography. Encyclopedia of Materials: Science and Technology (Second Edition). 2001, 6441-6448.

[43] Vetter, A., Kirner, R., Opalevs, D., Scholz, M., Leisching, P., Scharf, T., Noell, W., Rockstuhl, C., & Voelkel, R., Printing sub-micron structures using talbot mask-aligner lithography with a 193 nm CW laser light source. Optics Express. 2018, 26, 17.

[44] University of Alberta. nanoFAB: Nanoscribe Photonic Professional GT. 2014

[45] Kira. Nanoscribe 3D printers used by five of top ten universities in the world. 3ders. 30 Nov 2015.

[46] Graham, M. V., & Mosier, A. P. Development of antifouling surfaces to reduce bacterial attachment. Soft Matter 2013. 9, 6235–6244.

[47] Burgoyne, Francesca. Rapid curing of PDMS for microfluidic applications. Royal Society of Chemistry. 2006.

[48] Kooy, N., Mohamed, K., Pin, L. T., & Guan, O. S. (2014). A review of roll-to-roll nanoimprint lithography. Nanoscale research letters, 9(1), 320. https://doi.org/10.1186/1556-276X-9-320

[49] Wang, Zhixin, Alex A. Volinsky, and Nathan D. Gallant. "Nanoindentation study of polydimethylsiloxane elastic modulus using Berkovich and flat punch tips." Journal of Applied Polymer Science 132.5 (2015).

[50] Jin, Congrui, et al. "Mechanical characterization of crosslinking effect in polydimethylsiloxane using nanoindentation." Polymer Testing 56 (2016): 329-336.

[51] Singh, Akanksha, et al. "Low cost fabrication of polymer composite (h-ZnO+ PDMS) material for piezoelectric device application." Materials Research Express 3.7 (2016): 075702.

[52] Verma, Shatakshi, et al. "Development of multifunctional polydimethylsiloxane (PDMS)-epoxy-zinc oxide nanocomposite coatings for marine applications." Polymers for Advanced Technologies 30.9 (2019): 2275-2300.

[53] Carrillo, Fernando, et al. "Nanoindentation of polydimethylsiloxane elastomers: Effect of crosslinking, work of adhesion, and fluid environment on elastic modulus." Journal of materials research 20.10 (2005): 2820-2830.

[54] Nanoscribe GmbH. Printing Materials. Web 2020

[55] Menard, E.; Rogers, J. In Stamping Techniques for Micro- and Nanofabrication; Springer Handbook of Nanotechnology; Springer Berlin Heidelberg: Berlin, Heidelberg, 2010; pp 313-332.

[56] Lillian C. Hsu; Jean Fang; Diana A. Borca-Tasciuc; Randy W. Worobo; Carmen I. Moraru Effect of Micro- and Nanoscale Topography on the Adhesion of Bacterial Cells to Solid Surfaces. Applied and Environmental Microbiology 2013, 79, 2703-2712.

[57] Paulus H. S. Kwakman; Anje A. te Velde; Christina M. J. E. Vandenbroucke-Grauls; Sander J. H. van Deventer; Sebastian A. J. Zaat Treatment and Prevention of Staphylococcus epidermidis Experimental Biomaterial-Associated Infection by Bactericidal Peptide 2. Antimicrobial Agents and Chemotherapy 2006, 50, 3977-3983.

Appendix A: Photoresin Properties

IP-Dip	
Property	**Description**
Reactive group	acrylate
Curing mechanism	free radical polymerization (FRP)
Cured Polymer	thermoset
Polarity	hydrophobic
Hazard class	refer to the MSDS supplied with the shipment
Expiration date/shelf life and storage	warranted shelf life of 6 months from production
Chemical resistance	polymerized resin does not melt and cannot be dissolved
Biocompatibility	
Resist tone	negative
Polymerization	designed for 2PP
Solution set	3D SF
Development/washing	12 min Mr-Dev/30 s Novec
Pre/post bake	not required
Spin coating	not required
Removal/stripping	
95 % Material Loss	585 °C
Degredation Temp	371 °C
Color	yellow fluorescent (liquid; polymerized)
Fluorescence	yes
Refractive index (liquid)	1.521 @ 589 nm, 20°C
Refractive index (2PP polymerized)	1.552 @ 589 nm, 20°C
Transmittance (polymerized)	>95% @ at 633 nm and essentially transparent up to 2.4 µm with two local transmission minima at 2.9 µm and 3.4 µm
Dielectric constant (relative permittivity)/loss tangent	1.8/0.12
Young's modulus	2.91 GPa
Vickers Hardness	12.05 HV0.0025
Hardness	130.13 MPa
Storage modulus	3.17 GPa
Loss modulus	0.24 GPa
Poisson's ratio (estimated)	0.3 GPa
Expansion coefficient (2PP polymerized)	$5\text{-}8 \cdot 10^{-5}$ K^{-5}

Shrinkage after polymerization	5-17%
Density (liquid)	1.170 g/cm³ @ 20°C
Viscosity η (liquid)	2420 mPas @ 20°C

IP-S	
Property	**Description**
Reactive group	methacrylate
Curing mechanism	free radical polymerization (FRP)
Cured Polymer	thermoset
Polarity	hydrophobic
Hazard class	refer to the MSDS supplied with the shipment
Expiration date/shelf life and storage	warranted shelf life of 6 months from production
Chemical resistance	polymerized resin does not melt and cannot be dissolved
Cytotoxity	After 72h incubation, 2.0% inhibition of L929 mouse fibroblast cell growth by a UV-cured *IP-S* sample. UV-cured *IP-S* is therefore considered to be non-cytotoxic according to ISO10993-5.
Resin tone	negative
Polymerization	designed for 2PP; UV flood curing is possible
Solution set	3D MF
Developer/washing	20 min Mr-Dev/30 s Novec
Pre/post bake	not required
Spin coating	not required
Removal/stripping	
95 % Material Loss	549 °C
Degradation Temp	286 °C
Color	colorless (liquid); greenish (solid printing); yellowish (shell and scaffold printing)
Fluorescence	yes
Refractive index (liquid)	1.486 @ 589 nm, 20°C
Refractive index (2PP polymerized)	1.515 @ 589 nm, 20°C
Transmittance (polymerized)	2PP Transmittance >95% from 633 nm to 2.4 µm. Two local transmission minima at 2.9 and 3.4 µm.
Young's modulus	5.11 GPa
Vickers Hardness	20.68 HV0.0025
Hardness	223.33 MPa
Storage modulus	5.33 GPa

Loss modulus	0.26 GPa
Young's modulus	4.68 GPa
Vickers Hardness	20.29 HV0.0025
Hardness	219.11 MPa
Storage modulus	5.03 GPa
Loss modulus	0.27 GPa
Poisson's ratio (estimated)	0.3 GPa
Expansion coefficient (2PP polymerized)	
Shrinkage after polymerization	2-12%
Density (liquid)	1.111 g/cm³ @ 20°C
Swelling	Weight Increase %
purified water	1.5

Appendix B: Step by Step Bacteria Growth Procedure

Materials:

- 3 g TSA powder
- 100 mL DI water
- 2 Sterile 250 mL media bottle
- 2 petri dishes
- Inoculating loops
- *S. epidermidis 1457* stock solution
- pipette controller with a serological pipette
- 4.5 g TSB powder
- 1.5 grams of glucose
- 150 mL of DI water
- 100 mL sterilized beaker with a stir bar
- 10 mL syringe
- Syringe filter
- 100 mL Erlenmeyer flask
- Aluminum foil
- 70% ethanol
- 6-well plate with lid
- parafilm
- 2 pairs of sterile tweezers
- PDMS surface, about 2.5 x 3 cm
- Micropipette suitable for 0.2 μL
- Paper towels

- 0.5 µL of a solution of SYTO 9 at a concentration of 5 mM in DMSO
- Centrifuge tube
- Glass slide
- Cover slip

Procedures:

Preparing Agar Plates

1. Add 100 ml DI water to a sterile 250 mL media bottle
2. Weigh out 3 grams of TSA powder and add it to media bottle
3. Cover the media bottle with its lid and shake the bottle to mix
4. Make sure the lid is loosely attached, attach one piece of autoclave tape between the lid and bottle, and autoclave on the long liquid cycle (30 minutes)
5. Open the bag of sterile petri dishes in the hood. Open the bottle of agar solution in the hood and pour enough solution (about 15 mL) to coat the bottom of a sterile petri dish. Allow it to cool until it is set. Keep in the hood to remain sterile.
6. Store in refrigerator until use.

Streaking a Plate:

1. Take the stock solution of *S. epidermidis 1457* out of the -80 freezer. Take a sterile inoculating loop out of its bag, being careful not to touch any other surfaces with the end of the loop, and dip it into the stock solution. Place the stock back in the freezer, making sure to not leave it out for too long.
2. With the loop parallel to the surface of the Agar plate, gently swipe the loop back and forth on the agar taking up ¼ of the plate
3. Take a new inoculating loop and swipe through the previously streaked section once then swipe back and forth approximately 3 times in an area that has not be swiped before
   - This is performing a serial dilution on the plate with the bacteria stock
4. Label the streaked plate and let it incubate upside down with the agar on top to prevent condensation for 18-24 hours

Preparation of a TSB solution

1. Prepare a tryptic soy broth (TSB) solution by adding 4.5 grams of TSB powder to 150 mL of DI water in a sterile media bottle
2. Autoclave the solution and let cool

Glucose solution preparation

1. Take a sterilized beaker with a stir bar into the hood and pour 10-15 mL of media into the beaker so that the glucose will dissolve easier when heated
2. Place the beaker on a hotplate at 37-38 °C and turn on mixing
3. Place a dish on the balance and measure 1.5 g of glucose
4. Add the glucose to the beaker and turn up the hotplate and mixing to dissolve the glucose

5. Take the beaker of glucose solution, the beaker of TSB solution, a 10 mL syringe, and syringe filter to the hood. Pull up and push down on the syringe once before use
6. Suck up as much glucose solution as possible from the beaker
7. Secure the syringe to the filter and push out the glucose solution through the filter into the media bottle of TSB. Add "with 1% glucose" to the label on the bottle

Preparation of an overnight liquid culture:

1. Use the pipette controller with a serological pipette to measure 10 – 12 mL of TSB_g solution into a sterile 100 mL Erlenmeyer flask
2. Use an inoculating loop to place one colony of bacteria from the agar plate and stir it to the flask
3. Label the flask and then place in the incubator overnight while shaking at 200 rpm

Characterizing bacteria concentration

1. Add 970 µL media and 30 µL of overnight bacteria solution to a cuvette
2. Use a spectrophotometer to measure the absorbance of the bacteria sample by adding
   - This will determine the optical density at wavelength of light at 600 nm
3. Dilute the inoculum solution according to the McFarland Standard No. 0.5 to approximately 1.5×10^8 CFU/ml with TSB_g media. On the spectrophotometer used this was equivalent to an OD600 reading of 0.1
4. Further dilute the solution to 5×10^5 CFU/ml by adding 0.04 mL of bacterial suspension to 11.96 mL of TSB_g media

Culturing of Bacteria on PDMS Surface:

1. In the hood, sterilize the PDMS surface and two pairs of tweezers by soaking in 70% ethanol, enough to cover the items, in a petri dish for 10 minutes.
2. Rinse the PDMS surfaces three times with sterile water and dispose of the ethanol properly. Let the surfaces and tweezers air dry
3. Use tweezers to place the surface on the bottom of a 6-well plate. Cover the unused wells with parafilm
4. Use a micropipette to add the bacteria culture to the well so that the PDMS surface is submerged, about 0.75 mL.
5. Cover the used well plate with parafilm and incubate for 6 hours while shaking at 60 rpm
   - This will test initial bacterial adhesion

Bacteria Preparation for Imaging:

1. Take the surface out of the well with the bacteria suspension and place it in an empty well plate. Add about 6 mL of media and swirl the surfaces around with tweezers for 30 seconds
2. Wipe the bottom of the surface dry with a paper towel and place on a glass slide
3. Use a micropipette to add 0.5 µL of a solution of SYTO 9 at a concentration of 5 mM in DMSO to 50 µL of media in a centrifuge tube and combine using the micropipette
4. Micropipette less than 5 µL of the solution on the center of the surface
5. Incubate the surface with Syto 9 for 5 minutes to allow stain to absorb into the bacterial cells
6. Place a coverslip on the surface

Microscopy:

1. Uncover, turn on the fluorescence (be sure it is kept on for at least 15 minutes), and log onto the computer
2. Load the sample by placing it flat on the stage and push it into place. Move the stage with the knobs on the lower right to center the sample under the lens
3. Try to focus the microscope using the bright field. Make sure the fluorescence is off and turn on the bright field with the red switch on the left. A yellow-green light will appear
4. Switch to the fluorescence and use that to further focus it, first on the 10x, then 20x, and finally 40x. Be sure to not allow the lens to touch the sample
5. Once in focus, view the image on the computer and use the fine adjustment to further focus it
6. Adjust the exposure and acquire the image, choose a folder, and name the image (e.g. CTRL_Sample1_40x)
7. Move the stage and image another part of the sample
8. Repeat steps 5-7 two more times
9. Lower the stage, turn the objectives to 5x, and remove the sample
10. Close the software before signing out of the computer
11. Wipe down the stage

Image Analysis:

1. Find out the pixel sizes for each objective to determine the areas imaged
2. Convert the image type to 16-bit grayscale and upload the images to the ImageJ toolbox
3. Adjust the threshold of the images to distinguish cells from the background
4. Obtain the cell count of each topography using data obtained from ImageJ
5. Take the averages and standard deviations of the cell count for each of the 9 topographies and the control
6. Compare the cell count of the modified surfaces to the control surface to ensure the modified surface has a 50% decrease in cell adhesion

Appendix C: Full Nano Indenter Results

Table 7: Sample 1 5:1 PDMS Stiffness Results

	FREQUENCY	MODULUS STORAGE	MODULUS LOSS	LOSS FACTOR	STIFFNESS
	Hz	MPa	MPa	None	N/m
Test 1					
1:1	200	38.289933	8.729734	0.22799	3820
1:2	83	34.098922	6.747656	0.197885	3410
1:3	35	31.029284	5.186507	0.167149	3100
1:4	15	28.75678	3.985352	0.138588	2870
1:5	6	26.214875	2.943202	0.112272	2620
1:6	3	25.144045	2.394492	0.095231	2510
1:7	1	23.817374	1.729987	0.072635	2380
Test 2					
2:1	200	38.589093	8.799848	0.22804	3850
2:2	83	34.363392	6.814172	0.198297	3430
2:3	35	31.254149	5.224521	0.167162	3120
2:4	15	28.93925	4.015678	0.138762	2890
2:5	6	26.390388	2.963886	0.112309	2640
2:6	3	25.309338	2.419144	0.095583	2530
2:7	1	23.976516	1.749952	0.072986	2390
Test 3					
3:1	200	37.875282	8.557184	0.225931	3780
3:2	83	33.80612	6.612	0.195586	3380
3:3	35	30.79349	5.047814	0.163925	3070
3:4	15	28.567106	3.873106	0.135579	2850
3:5	6	26.099874	2.85865	0.109527	2610
3:6	3	25.031887	2.314921	0.092479	2500
3:7	1	23.788811	1.670961	0.070241	2380
Test 1					
Avg	49	2.227263	0.833177	0.333785	223
StdDev	67.17	0.807652	0.56147	0.116714	80.7
CoV	1.3707	0.362621	0.67389	0.349668	0.36275
Test 2					
Avg	49	2.255828	0.82031	0.324211	225
StdDev	67.17	0.798362	0.554554	0.116579	79.7
CoV	1.3707	0.353911	0.67603	0.359579	0.35383
Test 3					
Avg	49	2.403305	0.860532	0.319468	240

StdDev	67.17	0.842875	0.579762	0.11487	84.2
CoV	1.3707	0.350715	0.673725	0.359567	0.35066
Test 4					
Avg	49	2.304525	0.837953	0.323818	230
StdDev	67.17	0.822019	0.56888	0.116418	82.1
CoV	1.3707	0.356698	0.678892	0.359516	0.35669
Test 5					
Avg	49	2.264967	0.826041	0.325183	226
StdDev	67.17	0.807832	0.55779	0.115894	80.7
CoV	1.3707	0.356664	0.675256	0.356395	0.35657
Sample Statistics					
Avg	49	2.291178	0.835603	0.325293	229
StdDev	67.17	0.818193	0.564733	0.116191	81.7
CoV	1.3707	0.357106	0.675839	0.357189	0.35708

Table 2: Sample 2 5:1 PDMS Stiffness Results

	FREQUENCY	MODULUS STORAGE	MODULUS LOSS	LOSS FACTOR	STIFFNESS
	Hz	MPa	MPa	None	N/m
Test 1					
1:1	200	4.502074	0.667068	0.148169	450
1:2	83	4.079005	0.639133	0.156688	408
1:3	35	3.715913	0.591237	0.159109	371
1:4	15	3.404771	0.511207	0.150144	340
1:5	6	3.034361	0.443619	0.146199	303
1:6	3	2.855479	0.40144	0.140586	285
1:7	1	2.610437	0.342495	0.131202	261
Test 2					
2:1	200	4.908946	0.72845	0.148392	490
2:2	83	4.460809	0.698186	0.156515	446
2:3	35	4.063437	0.633124	0.15581	406
2:4	15	3.727024	0.546374	0.146598	373
2:5	6	3.328694	0.48043	0.14433	332
2:6	3	3.130114	0.433982	0.138647	313
2:7	1	2.882885	0.361517	0.125401	288
Test 3					
3:1	200	9.373178	1.356843	0.144758	936

3:2	83	8.570845	1.260337	0.147049	856
3:3	35	7.886025	1.140281	0.144595	787
3:4	15	7.303794	1.008724	0.13811	730
3:5	6	6.585205	0.867548	0.131742	658
3:6	3	6.232465	0.794768	0.127521	622
3:7	1	5.756397	0.688723	0.119645	574
Test 4					
4:1	200	4.775346	0.712027	0.149105	477
4:2	83	4.34434	0.67619	0.155648	434
4:3	35	3.962471	0.613535	0.154836	396
4:4	15	3.644197	0.53733	0.147448	364
4:5	6	3.253112	0.462031	0.142028	325
4:6	3	3.073318	0.413969	0.134698	307
4:7	1	2.805448	0.344756	0.122888	280
Test 5					
5:1	200	4.518478	0.589522	0.130469	451
5:2	83	4.103875	0.591907	0.144231	410
5:3	35	3.766254	0.538782	0.143055	376
5:4	15	3.476966	0.481977	0.13862	347
5:5	6	3.101393	0.411275	0.13261	310
5:6	3	2.937417	0.378225	0.128761	293
5:7	1	2.67171	0.322315	0.12064	267
	Hz	MPa	MPa	None	N/m
Test Statistics					
Test 1					
Avg	49	3.457435	0.513743	0.147443	345
StdDev	67.17	0.633128	0.114703	0.008797	63.2
CoV	1.3707	0.183121	0.22327	0.059665	0.18303
Test 2					
Avg	49	3.785987	0.554581	0.145099	378
StdDev	67.17	0.681569	0.127842	0.009917	68.1
CoV	1.3707	0.180024	0.23052	0.068343	0.18012
Test 3					
Avg	49	7.386844	1.016746	0.136203	737
StdDev	67.17	1.209311	0.229739	0.00952	121
CoV	1.3707	0.163711	0.225955	0.069893	0.16375
Test 4					
Avg	49	3.694033	0.53712	0.143807	369
StdDev	67.17	0.658566	0.12738	0.010869	65.8
CoV	1.3707	0.178278	0.237154	0.07558	0.17831
Test 5					
Avg	49	3.51087	0.473429	0.134055	351
StdDev	67.17	0.613422	0.098286	0.007822	61.3

CoV	1.3707	0.174721	0.207605	0.058352	0.17476
Sample Statistics					
Avg	49	4.367034	0.619124	0.141321	436
StdDev	67.17	1.709269	0.248794	0.010794	171
CoV	1.3707	0.391403	0.401849	0.076382	0.3911

Table 3: 20:1 Sample 1 PDMS Stiffness Results

	FREQUENCY	MODULUS STORAGE	MODULUS LOSS	LOSS FACTOR	STIFFNESS
	Hz	MPa	MPa	None	N/m
Cycle 1					
1:1	200	4.493753	1.582655	0.35219	449
2:1	200	4.397292	1.489645	0.338764	439
3:1	200	4.720707	1.70753	0.361711	471
4:1	200	4.511401	1.659259	0.367792	451
5:1	200	4.668846	1.633019	0.349769	466
Cycle 2					
1:2	83	3.739812	1.176173	0.314501	374
2:2	83	3.676087	1.122228	0.305278	367
3:2	83	3.923027	1.259284	0.320998	392
4:2	83	3.734031	1.233442	0.330324	373
5:2	83	3.894166	1.215212	0.31206	389
Cycle 3					
1:3	35	3.215007	0.876398	0.272596	321
2:3	35	3.177178	0.836924	0.263417	317
3:3	35	3.358863	0.936552	0.27883	336
4:3	35	3.181693	0.915484	0.287735	318
5:3	35	3.350259	0.906379	0.27054	335
Cycle 4					
1:4	15	2.843842	0.636423	0.22379	284
2:4	15	2.821302	0.603802	0.214016	282
3:4	15	2.953509	0.679766	0.230155	296
4:4	15	2.78748	0.66683	0.239223	279
5:4	15	2.959097	0.653701	0.220912	296
Cycle 5					
1:5	6	2.457714	0.45666	0.185807	245
2:5	6	2.448962	0.434057	0.177241	245
3:5	6	2.55425	0.490917	0.192196	255
4:5	6	2.390033	0.476078	0.199193	239
5:5	6	2.571039	0.469333	0.182546	257
Cycle 6					
1:6	3	2.289019	0.361527	0.15794	229

44

2:6	3	2.290604	0.341857	0.149243	229
3:6	3	2.382659	0.380505	0.159698	238
4:6	3	2.236781	0.376772	0.168444	223
5:6	3	2.40457	0.370607	0.154126	240
Cycle 7					
1:7	1	2.100919	0.245549	0.116877	210
2:7	1	2.113235	0.230159	0.108913	211
3:7	1	2.187269	0.26436	0.120863	218
4:7	1	2.031724	0.251943	0.124005	203
5:7	1	2.214048	0.255164	0.115248	221
Cycle Statistics					
Cycle 1					
Avg	200	4.5583999	1.6144215	0.3540453	455
StdDev	0	0.119068	0.0743018	0.0100297	11.9
CoV	0	0.026120561	0.046023805	0.028328976	0.02608
Cycle 2					
Avg	83	3.7934248	1.2012677	0.3166321	379
StdDev	0	0.097073	0.0479008	0.008496	9.58
CoV	0	0.025589809	0.039875244	0.026832317	0.02529
Cycle 3					
Avg	35	3.2566	0.894347	0.2746236	325
StdDev	0	0.081091	0.0346191	0.0081972	8.14
CoV	0	0.024900501	0.038708753	0.029848705	0.02501
Cycle 4					
Avg	15	2.8730462	0.6481046	0.2256193	287
StdDev	0	0.0703292	0.0263953	0.0085533	7.12
CoV	0	0.024478957	0.04072687	0.03791021	0.02481
Cycle 5					
Avg	6	2.4843997	0.4654087	0.1873965	248
StdDev	0	0.0682033	0.0191801	0.0076339	6.77
CoV	0	0.027452634	0.041211299	0.040736378	0.0273
Cycle 6					
Avg	3	2.3207266	0.3662537	0.1578901	232
StdDev	0	0.0629679	0.0137858	0.006381	6.27
CoV	0	0.027132842	0.037640132	0.040414476	0.02704
Cycle 7					
Avg	1	2.129439	0.249435	0.1171811	213
StdDev	0	0.0650033	0.0113889	0.0051441	6.47
CoV	0	0.03052602	0.045658779	0.04389837	0.0304

	FREQUENCY	MODULUS STORAGE	MODULUS LOSS	LOSS FACTOR	STIFFNESS
Sample Statistics					
Avg	49	3.0594337	0.777034	0.2333411	306
StdDev	67.17	0.8149027	0.4576628	0.0801839	81.4
CoV	1.3707	0.266357349	0.588986842	0.343633946	0.26635

Table 4: Sample 2 20:1 PDMS Stiffness Results

	FREQUENCY	MODULUS STORAGE	MODULUS LOSS	LOSS FACTOR	STIFFNESS
	Hz	MPa	MPa	None	N/m
Test 1					
1:1	200	4.709701	0.702247	0.149106	470
1:2	83	4.26409	0.670204	0.157174	426
1:3	35	3.88169	0.618454	0.159326	388
1:4	15	3.558137	0.535817	0.150589	356
1:5	6	3.155799	0.460104	0.145796	315
1:6	3	2.969519	0.422007	0.142113	297
1:7	1	2.693575	0.345835	0.128393	269
Test 2					
2:1	200	4.803236	0.715679	0.148999	480
2:2	83	4.356885	0.691703	0.158761	436
2:3	35	3.968166	0.631694	0.15919	396
2:4	15	3.628862	0.545186	0.150236	363
2:5	6	3.224033	0.466114	0.144575	322
2:6	3	3.039762	0.423373	0.139278	304
2:7	1	2.735343	0.358561	0.131084	273
Test 3					
3:1	200	4.644817	0.68305	0.147056	464
3:2	83	4.2078	0.661878	0.157298	420
3:3	35	3.833305	0.601248	0.156848	383
3:4	15	3.511537	0.531166	0.151263	351
3:5	6	3.12594	0.462996	0.148114	312
3:6	3	2.927452	0.408815	0.139649	292
3:7	1	2.705084	0.351498	0.12994	270
Test 4					
4:1	200	4.158306	0.602769	0.144956	415
4:2	83	3.775714	0.5919	0.156765	377
4:3	35	3.43669	0.543695	0.158203	343
4:4	15	3.156294	0.469179	0.148649	315
4:5	6	2.78779	0.409014	0.146716	278
4:6	3	2.628076	0.373861	0.142257	263
4:7	1	2.364602	0.30963	0.130944	236

Test 5					
5:1	200	4.582185	0.672168	0.146692	458
5:2	83	4.160691	0.644283	0.15485	416
5:3	35	3.784808	0.591233	0.156212	378
5:4	15	3.471646	0.521929	0.150341	347
5:5	6	3.080822	0.451133	0.146433	308
5:6	3	2.884603	0.406342	0.140866	288
5:7	1	2.671749	0.346916	0.129846	267
Test Statistics					
Test 1					
Avg	49	3.604645	0.536381	0.1475	360
StdDev	67.17	0.672928	0.123845	0.009581	67.3
CoV	1.3707	0.186684	0.230891	0.064957	0.18684
Test 2					
Avg	49	3.67947	0.547473	0.147446	368
StdDev	67.17	0.688235	0.127561	0.009402	68.8
CoV	1.3707	0.187047	0.232999	0.063767	0.18711
Test 3					
Avg	49	3.565134	0.528665	0.147167	356
StdDev	67.17	0.653861	0.117668	0.009003	65.4
CoV	1.3707	0.183404	0.222575	0.061174	0.18353
Test 4					
Avg	49	3.186782	0.471435	0.146927	318
StdDev	67.17	0.597783	0.104598	0.00852	59.7
CoV	1.3707	0.187582	0.221871	0.057987	0.18752
Test 5					
Avg	49	3.519501	0.519144	0.146463	352
StdDev	67.17	0.646675	0.114201	0.008349	64.6
CoV	1.3707	0.183741	0.219979	0.057003	0.18384
Sample Statistics					
Avg	49	3.511106	0.52062	0.147101	351
StdDev	67.17	0.674513	0.120742	0.008992	67.4
CoV	1.3707	0.192108	0.23192	0.061127	0.19219

Table 5: Sample 1 40:1 Stiffness Results

	FREQUENCY	MODULUS STORAGE	MODULUS LOSS	LOSS FACTOR	STIFFNESS
	Hz	MPa	MPa	None	N/m
Cycle 1					
1:1	200	3.466187	1.548806	0.446833	346
2:1	200	3.928208	1.857805	0.47294	393
3:1	200	3.646828	1.656688	0.454282	364

4:1	200	4.406248	2.189736	0.496962	440
5:1	200	3.355806	1.537682	0.458215	335
Cycle 2					
1:2	83	2.746631	1.105708	0.402569	274
2:2	83	3.095792	1.325606	0.428196	309
3:2	83	2.886418	1.181629	0.409376	288
4:2	83	3.411953	1.555185	0.455805	341
5:2	83	2.656767	1.099555	0.41387	265
Cycle 3					
1:3	35	2.267167	0.798511	0.352207	227
2:3	35	2.530842	0.94338	0.372754	253
3:3	35	2.376265	0.846443	0.356207	237
4:3	35	2.750469	1.0978	0.399132	275
5:3	35	2.186206	0.789884	0.361303	218
Cycle 4					
1:4	15	1.938059	0.55903	0.288448	194
2:4	15	2.142691	0.665086	0.310398	214
3:4	15	2.030911	0.599058	0.29497	203
4:4	15	2.313627	0.77168	0.333537	231
5:4	15	1.870337	0.551365	0.294795	187
Cycle 5					
1:5	6	1.624482	0.391346	0.240905	162
2:5	6	1.788377	0.454929	0.254381	179
3:5	6	1.695662	0.413021	0.243575	169
4:5	6	1.905641	0.520927	0.27336	190
5:5	6	1.552565	0.381275	0.245578	155
Cycle 6					
1:6	3	1.489891	0.296402	0.198942	149
2:6	3	1.632335	0.346231	0.212108	163
3:6	3	1.558157	0.317037	0.203469	156
4:6	3	1.731813	0.403267	0.232858	173
5:6	3	1.421744	0.288093	0.202634	142
Cycle 7					
1:7	1	1.346275	0.197264	0.146526	134
2:7	1	1.461154	0.229807	0.157278	146
3:7	1	1.398768	0.20663	0.147723	140
4:7	1	1.534625	0.262877	0.171297	153
5:7	1	1.289567	0.192157	0.149009	129
Cycle Statistics					
Cycle 1					
Avg	200	3.7606553	1.7581433	0.4658462	376
StdDev	0	0.3764134	0.244509	0.0177311	37.6

	Frequency	Modulus Storage	Modulus Loss	Loss Factor	Stiffness
CoV	0	0.100092507	0.139072284	0.038062076	0.10005
Cycle 2					
Avg	83	2.9595121	1.2535369	0.4219631	296
StdDev	0	0.2704037	0.1714176	0.0188902	27
CoV	0	0.091367653	0.136747176	0.044767502	0.09142
Cycle 3					
Avg	35	2.4221898	0.8952037	0.3683206	242
StdDev	0	0.2006998	0.1150527	0.0168797	20
CoV	0	0.082858836	0.128521238	0.04582878	0.08266
Cycle 4					
Avg	15	2.0591248	0.6292439	0.3044296	206
StdDev	0	0.1567471	0.0818279	0.0162516	15.6
CoV	0	0.076123169	0.130041601	0.053383771	0.07569
Cycle 5					
Avg	6	1.7133453	0.4322996	0.2515599	171
StdDev	0	0.1238282	0.0510277	0.0118007	12.3
CoV	0	0.072272759	0.118037919	0.046910087	0.0721
Cycle 6					
Avg	3	1.566788	0.3302057	0.210002	156
StdDev	0	0.1082174	0.0416756	0.0122158	10.8
CoV	0	0.069069615	0.12621104	0.058169953	0.06931
Cycle 7					
Avg	1	1.4060779	0.2177471	0.1543666	140
StdDev	0	0.0857463	0.0260006	0.0092677	8.54
CoV	0	0.060982624	0.119407444	0.06003685	0.06084
Sample Statistics					
Avg	49	2.2696705	0.7880543	0.3109269	227
StdDev	67.17	0.8132733	0.5304989	0.1065574	81.2
CoV	1.3707	0.358322215	0.673175565	0.342708863	0.35841

Table 6: Sample 2 40:1 PDMS Stiffness Results

	FREQUENCY	MODULUS STORAGE	MODULUS LOSS	LOSS FACTOR	STIFFNESS
	Hz	MPa	MPa	None	N/m
Test 1					
1:1	200	3.768984	1.892621	0.502157	376
1:2	83	2.937511	1.339026	0.455837	294

1:3	35	2.376179	0.950861	0.400164	237
1:4	15	1.992528	0.658427	0.330448	199
1:5	6	1.652271	0.440947	0.266873	165
1:6	3	1.505739	0.336308	0.223351	150
1:7	1	1.357629	0.214048	0.157663	136
Test 2					
2:1	200	3.777697	1.868025	0.494488	377
2:2	83	2.956884	1.318202	0.445808	295
2:3	35	2.404669	0.935061	0.388852	240
2:4	15	2.033938	0.647431	0.318314	203
2:5	6	1.685978	0.439664	0.260777	168
2:6	3	1.535641	0.324449	0.211279	153
2:7	1	1.39599	0.209339	0.149957	139
Test 3					
3:1	200	4.00476	1.954509	0.488047	400
3:2	83	3.149852	1.382958	0.439055	315
3:3	35	2.563659	0.9807	0.382539	256
3:4	15	2.167155	0.680844	0.314165	217
3:5	6	1.80168	0.458885	0.254698	180
3:6	3	1.646184	0.34545	0.209849	165
3:7	1	1.489844	0.220379	0.147921	149
Test 4					
4:1	200	3.869193	1.913379	0.494516	386
4:2	83	3.025513	1.349478	0.446033	302
4:3	35	2.464163	0.955118	0.387603	246
4:4	15	2.075379	0.657763	0.316936	208
4:5	6	1.717798	0.443777	0.25834	172
4:6	3	1.56808	0.334047	0.213029	157
4:7	1	1.41155	0.21211	0.150268	141
Test 5					
5:1	200	3.802648	1.877772	0.493806	380
5:2	83	2.975406	1.330204	0.447066	297
5:3	35	2.417335	0.941464	0.389463	242
5:4	15	2.043499	0.652598	0.319353	204
5:5	6	1.68824	0.441526	0.26153	169
5:6	3	1.535975	0.326601	0.212634	154
5:7	1	1.391668	0.212126	0.152426	139
Test Statistics					
Test 1					
Avg	49	2.227263	0.833177	0.333785	223
StdDev	67.17	0.807652	0.56147	0.116714	80.7
CoV	1.3707	0.362621	0.67389	0.349668	0.36275
Test 2					

Avg	49	2.255828	0.82031	0.324211	225
StdDev	67.17	0.798362	0.554554	0.116579	79.7
CoV	1.3707	0.353911	0.67603	0.359579	0.35383
Test 3					
Avg	49	2.403305	0.860532	0.319468	240
StdDev	67.17	0.842875	0.579762	0.11487	84.2
CoV	1.3707	0.350715	0.673725	0.359567	0.35066
Test 4					
Avg	49	2.304525	0.837953	0.323818	230
StdDev	67.17	0.822019	0.56888	0.116418	82.1
CoV	1.3707	0.356698	0.678892	0.359516	0.35669
Test 5					
Avg	49	2.264967	0.826041	0.325183	226
StdDev	67.17	0.807832	0.55779	0.115894	80.7
CoV	1.3707	0.356664	0.675256	0.356395	0.35657
Sample Statistics					
Avg	49	2.291178	0.835603	0.325293	229
StdDev	67.17	0.818193	0.564733	0.116191	81.7
CoV	1.3707	0.357106	0.675839	0.357189	0.35708

Appendix D: Full Bacteria Testing Results

5 Hour Growth Time Bacteria Adhesion Results

5:1					
Slice	Count	Total Area	Average Size	%Area	Mean
Image 1 Sample 1.tif	290	0.158	5.47E-04	0.29	255
Image 2 Sample 1.tif	321	0.136	4.25E-04	0.25	255
Image 3 Sample 1.tif	331	0.151	4.57E-04	0.277	255
Average	**314**	**0.148333**	**0.000476**	**0.272333**	

20:1					
Slice	Count	Total Area	Average Size	%Area	Mean
Image 1 Sample 2.tif	52	0.051	0.000986	0.094	255
Image 2 Sample 2.tif	81	0.064	0.000795	0.118	255
Image 3 Sample 2.tif	183	0.149	0.000814	0.273	255
Average	**105.3333**	**0.088**	**0.000865**	**0.161667**	

40:1					
Slice	Count	Total Area	Average Size	%Area	Mean
Image 1 Sample 3.tif	29	0.01	0.000354	0.019	255
Image 2 Sample 3.tif	29	0.018	0.00061	0.032	255
Image 3 Sample 3.tif	41	0.034	0.000827	0.062	255
Average	**33**	**0.020667**	**0.000597**	**0.037667**	

18-24 Hour Growth Time Bacteria Adhesion Results

5:1 Sample 2					
Slice	Count	Total Area	Average Size	%Area	Mean
Sample 2 Image 1	115	0.231	0.002	0.423	255
Sample 2 Image 2	477	0.022	4.67E-05	0.041	255
Sample 2 Image 3	28	0.028	9.82E-04	0.052	255
Sample 2 Image 4	479	7.335	0.015	13.431	255
Sample 2 Image 5	493	1.097	0.002	2.009	255
Sample 2 Image 6	138	0.264	0.002	0.484	255
Average	**288.3333**	**1.496167**	**0.00367145**	**2.74**	

5:1 Sample 3					
Slice	Count	Total Area	Average Size	%Area	Mean
Sample 3 Image 1	57	0.032	5.63E-04	0.059	255
Sample 3 Image 2	52	0.035	6.64E-04	0.063	255
Sample 3 Image 3	516	0.138	2.67E-04	0.252	255
Sample 3 Image 4	355	0.112	3.15E-04	0.205	255
Sample 3 Image 5	374	0.89	0.002	1.629	255
Sample 3 Image 6	98	0.125	0.001	0.229	255
Average	**242**	**0.222**	**0.0008013**	**0.406**	**255**

Sample 2 20:1					
Slice	Count	Total Area	Average Size	%Area	Mean
Sample 2 Image 1	4244	24.392	0.006	44.664	255
Sample 2 Image 2	1442	6.064	0.004	11.104	255
Sample 2 Image 3	3077	7.826	0.003	14.329	255
Sample 2 Image 4	5213	3.356	6.44E-04	6.145	255
Sample 2 Image 5	705	1.283	0.002	2.349	255
Sample 2 Image 6	1005	1.087	0.001	1.99	255
Average	**2614.333**	**7.334667**	**0.002774**	**13.43017**	

Sample 3 20:1					
Slice	Count	Total Area	Average Size	%Area	Mean
Sample 3 Image 1	3262	36.762	0.011	67.313	255
Sample 3 Image 2	3217	44.503	0.014	81.487	255
Sample 3 Image 3	2811	1.858	6.61E-04	3.403	255
Sample 3 Image 4	2446	3.135	0.001	5.74	255
Sample 3 Image 5	4332	14.774	0.003	27.052	255
Sample 3 Image 6	2105	1.654	7.86E-04	3.029	255
Average	**3028.833**	**17.11433**	**0.005075**	**31.33733**	

Sample 2 40:1					
Slice	Count	Total Area	Average Size	%Area	Mean
Sample 3 Image 1	3032	6.338	0.002	11.605	255
Sample 3 Image 2	5300	9.709	0.002	17.777	255
Sample 3 Image 3	3304	4.95	0.001	9.064	255
Sample 3 Image 4	324	0.495	0.002	0.907	255
Sample 3 Image 5	3581	26.816	0.007	49.102	255
Sample 3 Image 6	3038	7.152	0.002	13.096	255
Average	**3096.5**	**9.243333**	**0.002667**	**16.92517**	

Sample 3 40:1					
Slice	Count	Total Area	Average Size	%Area	Mean
Sample 3 Image 1	1905	8.486	0.004	15.538	255
Sample 3 Image 2	1822	14.949	0.008	27.373	255
Sample 3 Image 3	813	4.723	0.006	8.648	255
Sample 3 Image 4	1389	9.557	0.007	17.5	255
Sample 3 Image 5	2454	7.178	0.003	13.143	255
Sample 3 Image 6	4298	14.686	0.003	26.891	255
Average	**2113.5**	**9.929833333**	**0.005166667**	**18.18216667**	

Appendix E: Full Bacteria Testing Images
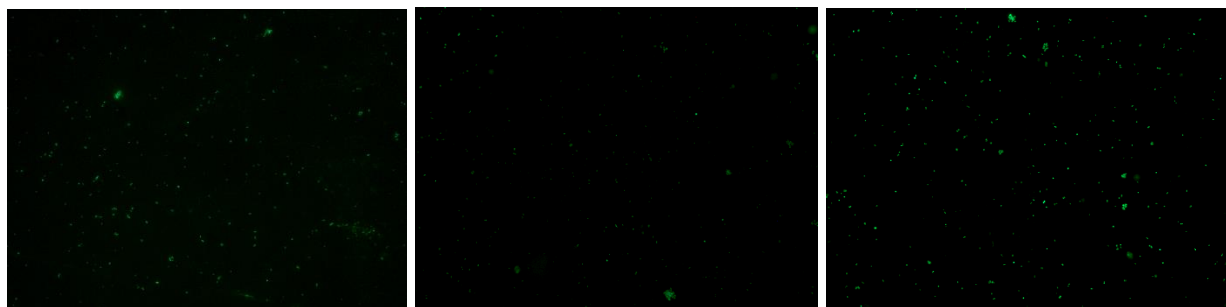
Sample 1 - 5:1 PDMS Images
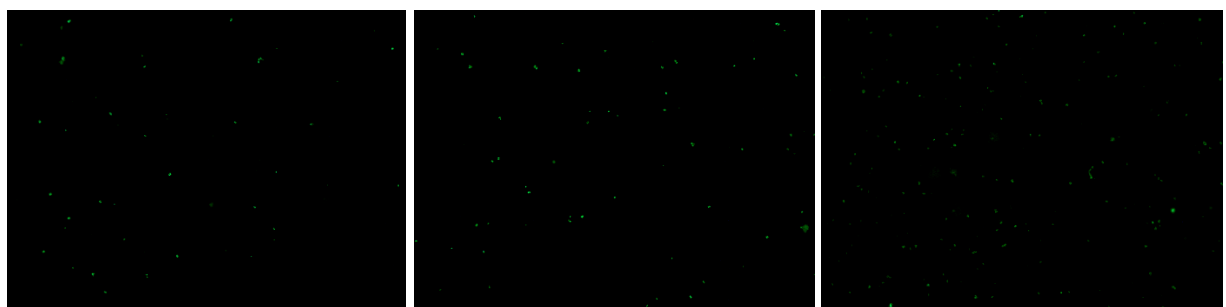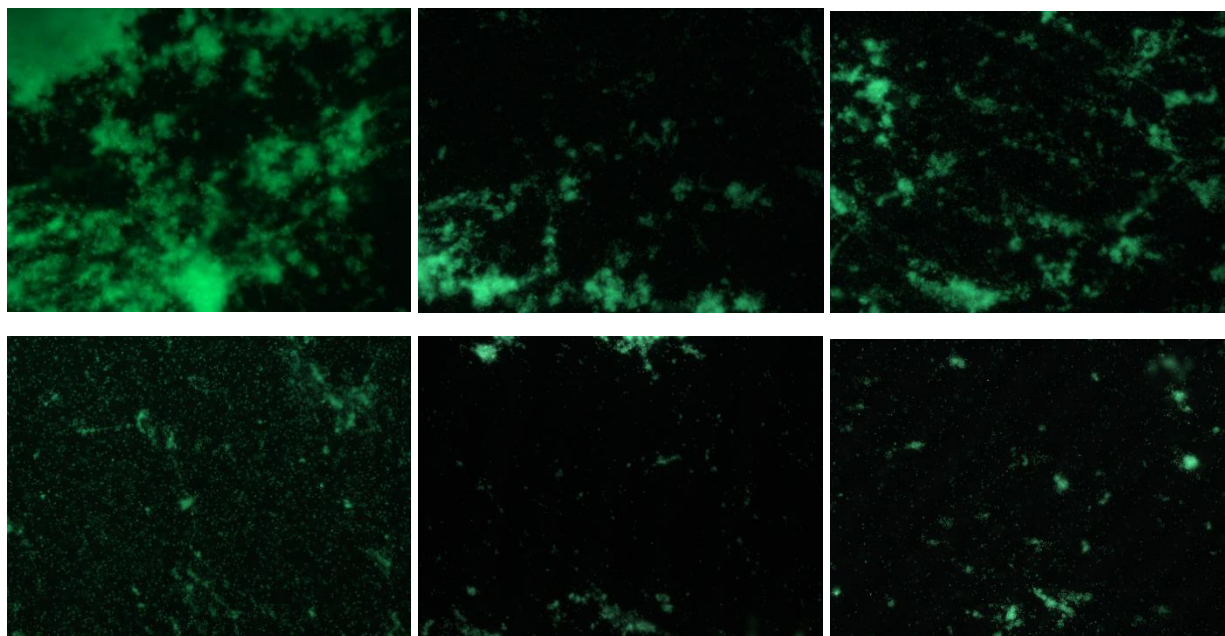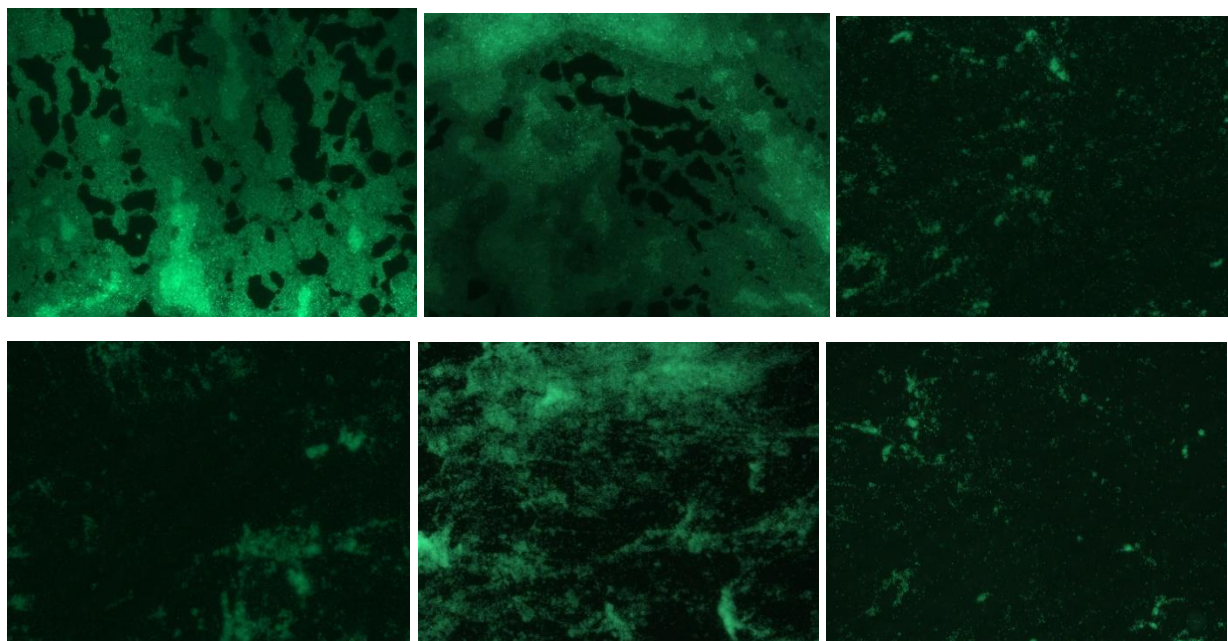

Sample 1 - 20:1 PDMS Images
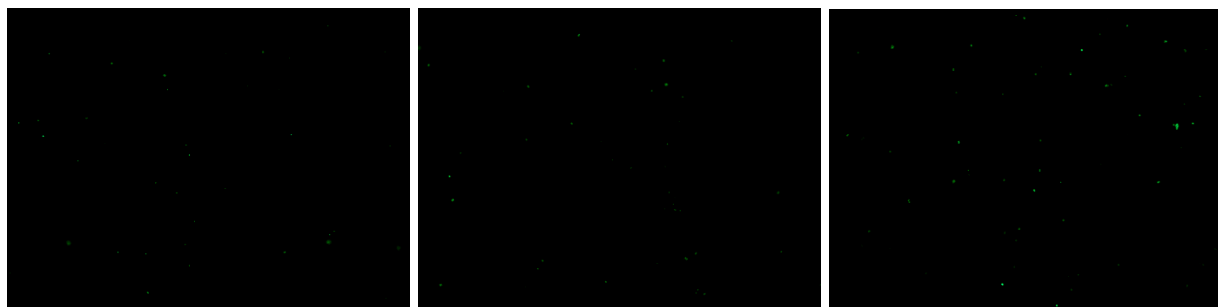
Sample 1 - 40:1 PDMS Images
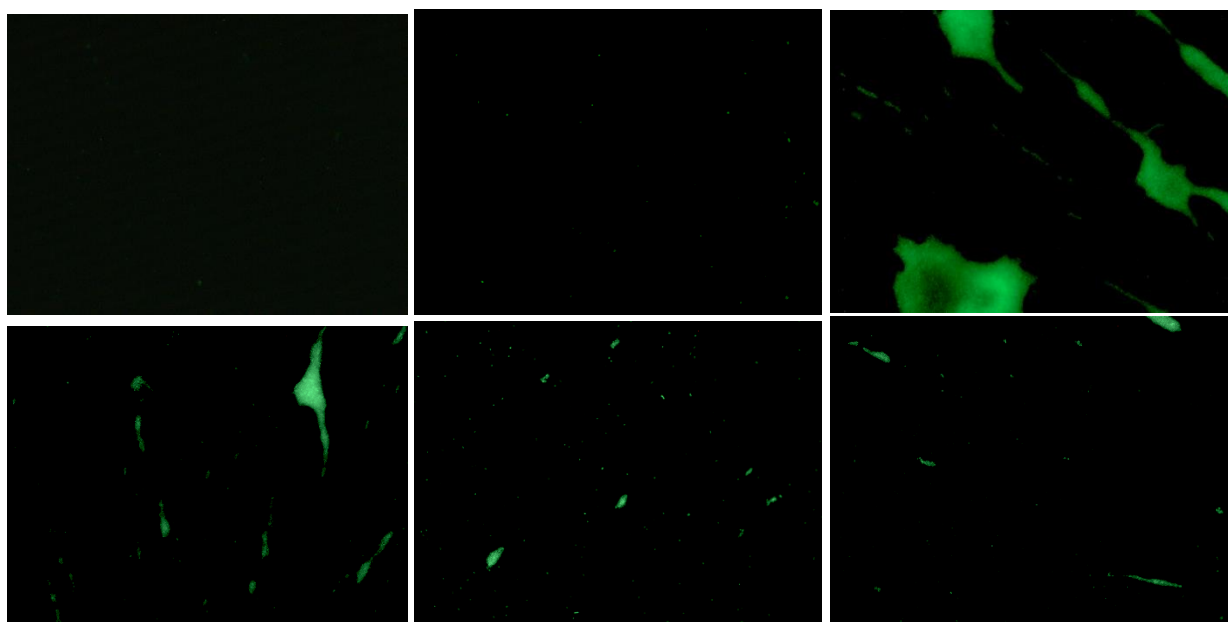
Sample 2 - 5:1 PDMS Images
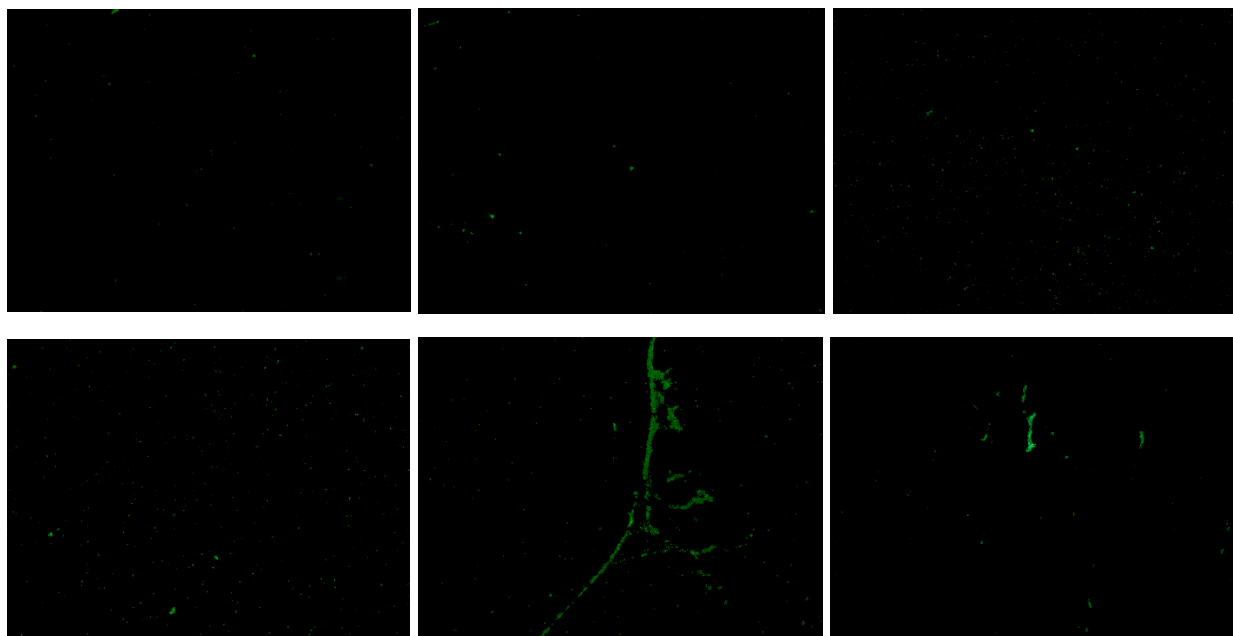
Sample 3 - 5:1 PDMS Images

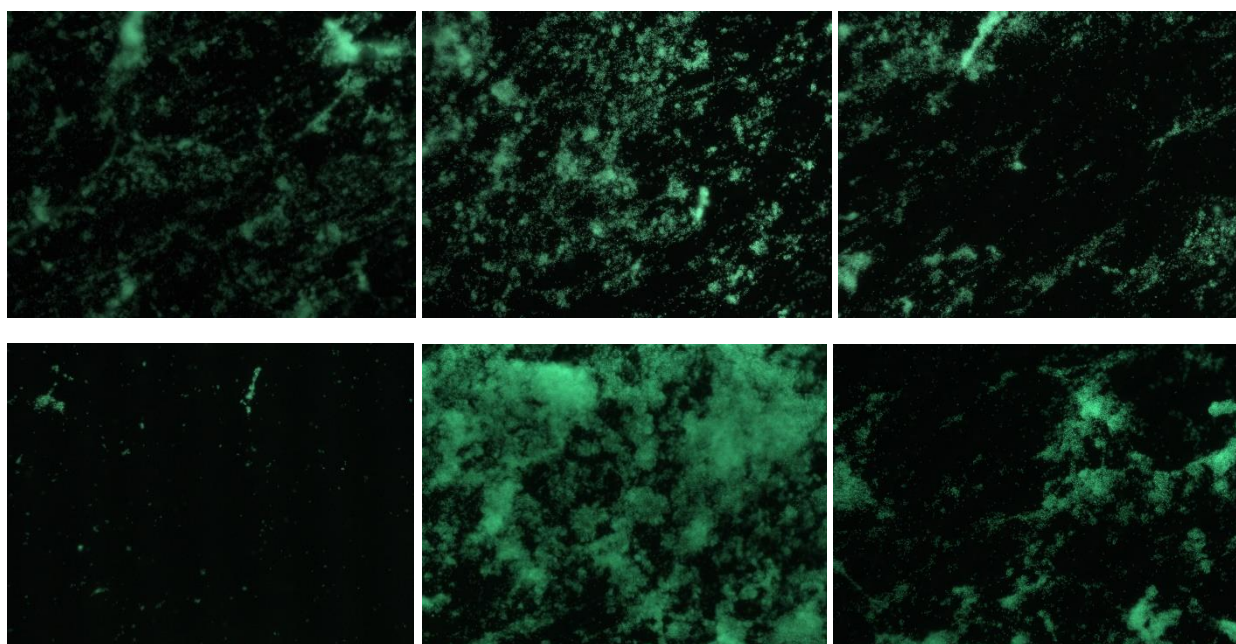*Sample 2 - 20:1 PDMS Images*

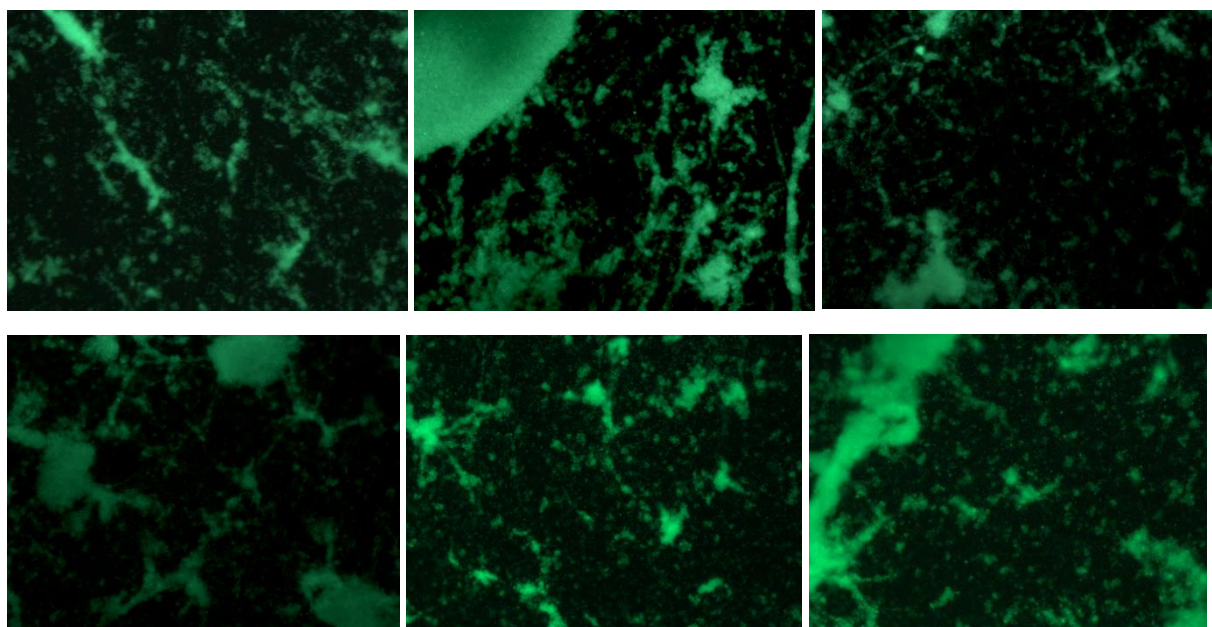*Sample 3 - 20:1 PDMS Images*

Sample 2 - 40:1 PDMS Images

Sample 3 - 40:1 PDMS Images